

SUMMER INTERNSHIP

Development of a Structural Health Monitoring Method for Damage Identification: A Case Study of the Livraria Lello



Louvain School of Engineering

Colin Cloos – colin.cloos@student.uclouvain.be

NCREP supervisor : Prof. Alexandre A. Costa
UCLouvain supervisor : Prof. Jean-Pierre Raskin

August 14, 2025

Contents

1	Introduction	4
1	Fast Fourier Transform Method (FFT)	4
1.1	Results	5
2	Part I : FDD-Based Tool for Tracking Structural Vibration Frequencies and Damage Detection	7
1	Frequency Domain Decomposition Method (FDD)	7
1.1	Results	8
2	Coherence Analysis [2]	9
2.1	Mathematical Definition of the Coherence Function	9
2.2	Mathematical Definition of the 3 Peack Picking (PP) indices	10
2.3	Results	10
3	Peak-Picking (PP) Method	11
3.1	Method 1	11
3.2	Method 2	12
4	Processing Multiple Files	14
4.1	Sensitivity Analysis with <code>nperseg = 1024</code>	14
4.2	Sensitivity Analysis with <code>nperseg = 512</code>	15
4.3	Results with a 60 min time window	16
3	Data Collection on "Alfredo" 2-Story Experimental Structure	18
1	Test <code>i = 0</code>	18
2	Test <code>i = 1</code>	19
3	Test <code>i = 1 bis</code>	19
4	Test <code>i = 2</code>	19
5	Test <code>i = 3</code>	20

4 Part II : Statistical Anomaly Detection for Damage Identification Using Temporal and Frequency Data	21
1 Overview of the Method	21
2 Results from the 4-Story Experimental Structure	22
3 Results from the "Alfredo" 2-Story Experimental Structure	24
3.1 Test $i = 0$	25
3.2 Test $i = 1$	26
3.3 Test $i = 1$ bis	26
3.4 Test $i = 2$	27
3.5 Test $i = 3$	28
4 Results from the Livraria Lello Staircase	29
5 Conclusion	32
1 Conclusion	32
2 Future Developments	32
A Part I: method 2 (details)	33
B "Alfredo" 2-Story Experimental Structure : configurations	34
1 Test $i = 0$	34
2 Test $i = 1$	36
3 Test $i = 1$ bis	38
4 Test $i = 2$	38
5 Test $i = 3$	40

Chapter 1

Introduction

Structural Health Monitoring (SHM) involves various methods to assess the condition of civil engineering structures over time. This report focuses on two complementary approaches to SHM, each playing a critical role in identifying potential damage in historic structures such as the Livraria Lello in Porto.

The first part of this study focuses on tracking the vibration frequencies of the structure over time using Frequency Domain Decomposition (FDD). A decrease in these vibration frequencies can signal potential structural damage, indicating that the structure may be becoming more flexible. In addition to identifying frequency modes, it is essential to determine the corresponding shape modes. This dual identification ensures the method's consistency by tracking the same modes over time.

The second part of the study introduces a statistical anomaly detection method based on both temporal and frequency domain data. By developing an anomaly detection index, this method enhances our ability to identify damage by detecting deviations from the normal behavior of the structure. This statistical approach complements the frequency tracking method by providing an additional layer of analysis for damage identification.

Together, these two approaches aim to develop a robust SHM method for the Livraria Lello. By monitoring both vibration frequencies and implementing statistical anomaly detection, we offer a comprehensive strategy for detecting structural changes, thereby ensuring the ongoing safety and preservation of this historic building.

The methods are applied to the staircase of Livraria Lello, using data collected from accelerometers located on the first and second levels. Initially, the method from Part I is applied to data recorded on July 10, 2023, between 4 AM and 5 AM. Figure 1.1 presents the time series data for this initial analysis, focusing solely on the staircase. The data is detrended to remove its DC component and then scaled, ensuring a clearer analysis of the oscillatory behavior and allowing frequency changes to be identified accurately.

1. Fast Fourier Transform Method (FFT)

To analyze the vibration frequencies of the staircase, we first employ the Fast Fourier Transform (FFT). The FFT is a key tool in civil engineering for analyzing vibration frequencies by transforming time-domain data into the frequency domain. This method reveals dominant frequencies and their amplitudes, making it essential for assessing and managing structural dynamics.

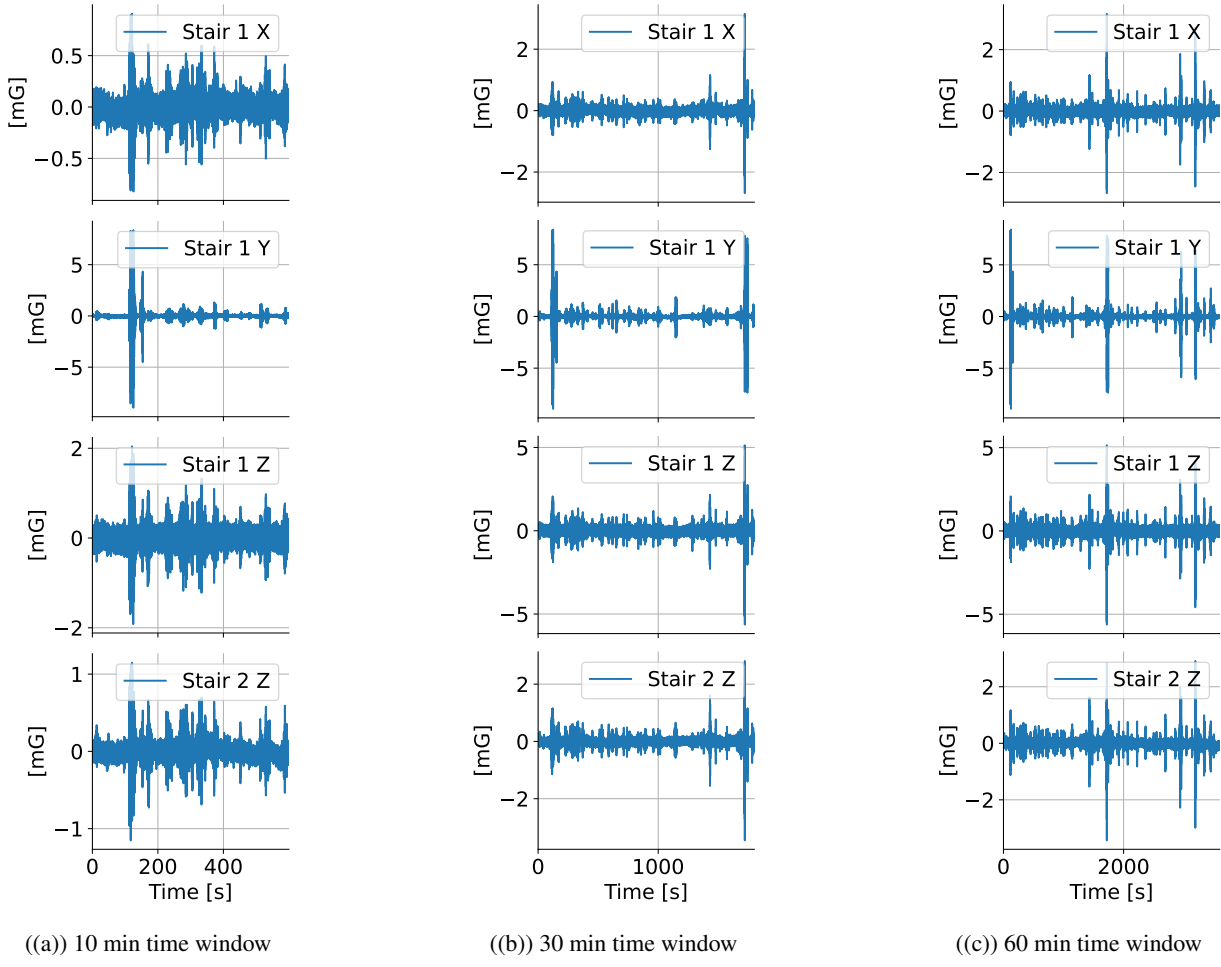


Figure 1.1. Time series data were collected from the staircase of Livraria Lello on July 10, 2023, between 4 AM and 5 AM. The data are from accelerometers, with the letters X, Y, or Z indicating the direction.

1.1. Results

Figure 1.2 displays the frequency domain signals obtained from applying the FFT to the staircase time series data. The frequency domain has been cropped to the range of 8 Hz to 24 Hz for clarity. The FFT identifies prominent peaks around frequencies of approximately 11 Hz, 16 Hz, and 22 Hz, corresponding to the primary vibration frequencies of the staircase.

It is observed that as the time window length increases, the amplitude of the frequency components also increases. This variation occurs because the amplitude obtained from the FFT is proportional to the length of the time window. A longer time window captures more data, potentially leading to higher amplitude values, which can skew the interpretation of the signal's strength and frequency components.

To address this issue, we use the power spectral density (PSD) method. The PSD provides a more accurate measure of the signal's power distribution across different frequencies and is less sensitive to the time window length. By normalizing the power with respect to the time window, the PSD offers a consistent representation of the signal's frequency content, mitigating the amplitude variation problem inherent in the FFT and providing a clearer understanding of the signal's spectral characteristics.

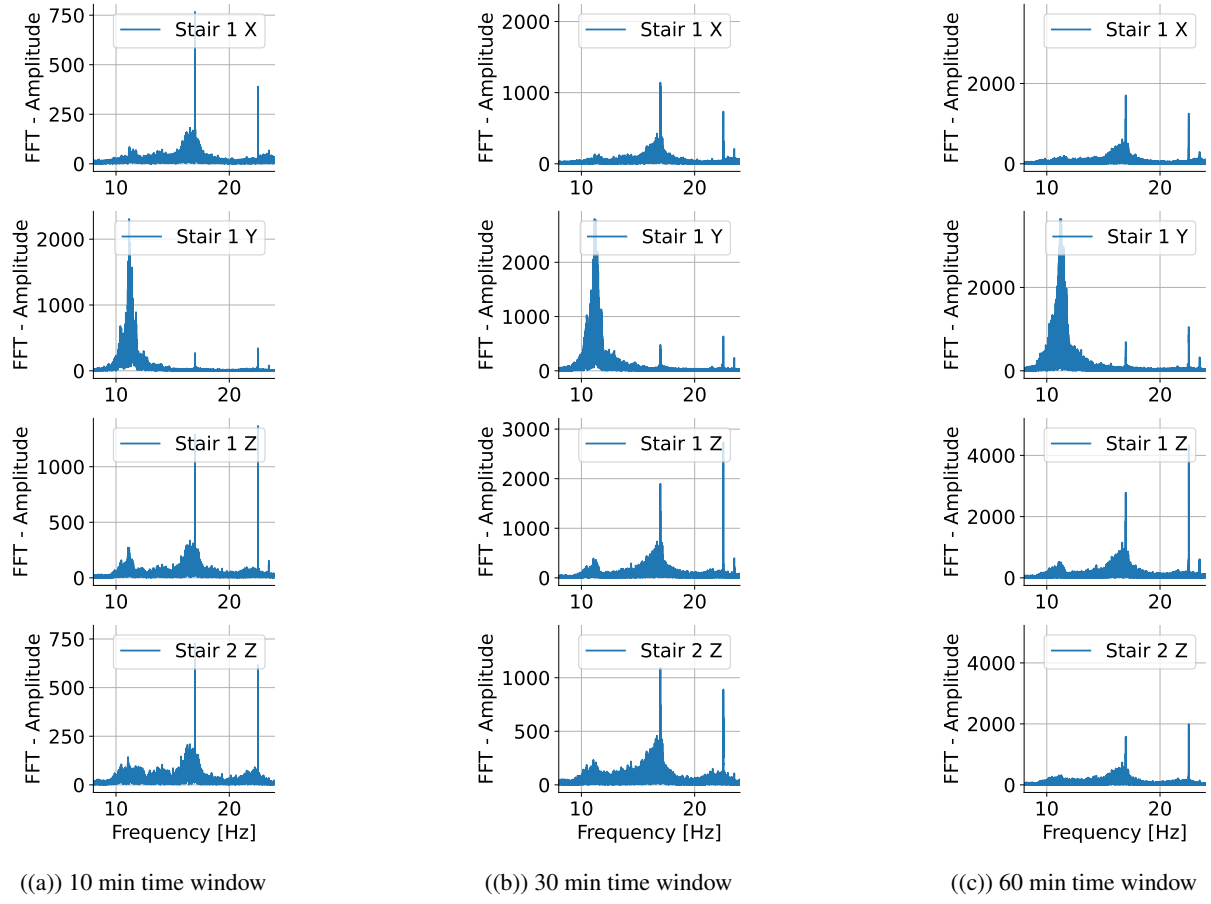


Figure 1.2. FFT of the staircase time series data shown in Figure 1.1. The time step is 0.01 s, and the real FFT is computed to obtain only positive frequencies, as the temporal signal is real-valued. The result shows the frequency spectrum of the signal, highlighting the dominant frequencies and their amplitudes.

Chapter 2

Part I : FDD-Based Tool for Tracking Structural Vibration Frequencies and Damage Detection

1. Frequency Domain Decomposition Method (FDD)

Frequency Domain Decomposition (FDD) is a technique used in Structural Health Monitoring (SHM) to identify the dynamic characteristics of structures. Unlike the Fast Fourier Transform (FFT), which provides a direct frequency-domain representation of a time-domain signal, FDD utilizes the cross-power spectral density (PSD) matrix obtained from multiple sensor signals. This approach allows for the extraction of mode shapes and frequencies, which are crucial for understanding the dynamic behavior of structures.

While the FFT is efficient and straightforward for spectral analysis, it has limitations when dealing with multi-channel data and extracting modal information. In this project, the FDD method was employed to identify the modal frequencies of the structure from the collected signals.

Mathematical Definition of FDD

Consider a structure instrumented with n sensors providing time-domain signals $\mathbf{x}(t) = [x_1(t), x_2(t), \dots, x_n(t)]^T$.

Power Spectral Density (PSD) Estimation

First, the PSD matrix $\mathbf{S}_{xx}(f)$, containing the PSD and the Cross PSD (CPSD), is estimated using Welch's method. For each segment of the time series, the discrete Fourier transform (DFT) is computed and averaged over multiple segments:

$$\mathbf{S}_{xx}(f) = \frac{1}{M} \sum_{k=1}^M \mathbf{X}_k(f) \mathbf{X}_k^H(f) \quad (2.1)$$

where $\mathbf{X}_k(f)$ is the DFT of the k -th segment, M is the number of segments, and H denotes the Hermitian transpose.

. SINGULAR VALUE DECOMPOSITION (SVD)

At each frequency f , the PSD matrix $\mathbf{S}_{xx}(f)$ is decomposed using SVD:

$$\mathbf{S}_{xx}(f) = \mathbf{U}(f)\boldsymbol{\Sigma}(f)\mathbf{U}^H(f) \quad (2.2)$$

where $\mathbf{U}(f)$ is a unitary matrix containing the singular vectors, and $\boldsymbol{\Sigma}(f)$ is a diagonal matrix containing the singular values.

. MODAL IDENTIFICATION

The peaks in the singular values $\sigma_i(f)$ of $\boldsymbol{\Sigma}(f)$ indicate the presence of structural modes. The corresponding singular vectors $\mathbf{u}_i(f)$ at these peak frequencies represent the mode shapes.

. MODE SHAPE EXTRACTION

For each identified frequency f_m , the mode shape Φ_m is extracted as the corresponding singular vector:

$$\Phi_m = \mathbf{u}_i(f_m)$$

where $\mathbf{u}_i(f_m)$ is the i -th column of the unitary matrix $\mathbf{U}(f_m)$ defined in 2.2, and i is the index of the significant singular value at f_m .

In practice, the collected time series are acceleration data, so the obtained mode shapes are in units of acceleration. To obtain displacement mode shapes, one needs to integrate the data twice, either in the time domain or the frequency domain, before applying the FDD method.

For a more detailed explanation of why the mode shapes are obtained this way, see p.59 of [1].

1.1. Results

Figure 2.1 presents the PSD obtained from the time series shown in Figure 1.1. Three modes are visually identified : one at a frequency of approximately 11 Hz, another at 16 Hz, and a third at approximately 22 Hz. As expected, the power of the signal does not increase further with the time window.

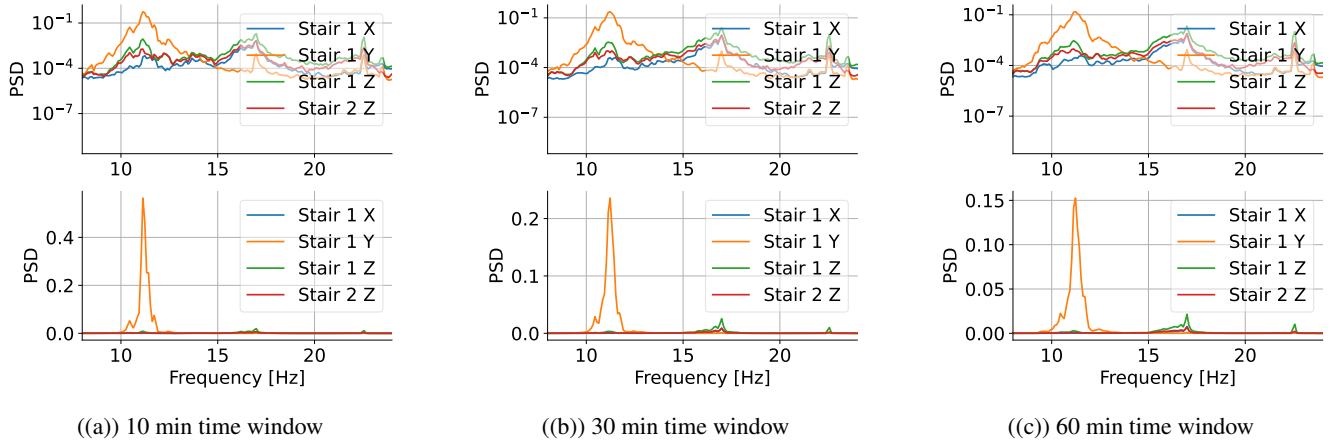


Figure 2.1. PSD results (diagonal entries of $\mathbf{S}_{xx}(f)$) using the Welch method obtained from the staircase time series data shown on Figure 1.1, with different time windows and the parameter `nperseg = 1024`. The plots above are presented on a semi-logarithmic scale, whereas the plots below are on a linear scale. In what follows, only the logarithmic plots will be presented.

Figure 2.2 shows the Singular Value Decomposition (SVD) of the PSD matrix represented by dotted lines. The singular values, $\sigma_1, \sigma_2, \sigma_3$, and σ_4 , correspond to the power concentration in the respective modes at each frequency.

In the context of vibration frequency picking, these singular values offer insights into the dominant frequencies. The largest singular value, σ_1 , typically signifies the most dominant frequency component at each frequency point, followed by σ_2 , σ_3 , and σ_4 , which represent successively less significant components. By examining the peaks in σ_1 , we can identify the primary vibration frequencies of the structure.

In our analysis, across all considered time windows, the peaks in σ_1 are observed at similar frequencies to those shown in Figure 2.1, indicating the stability and persistence of these frequency components.

The solid line and the annotated peaks with crosses will be explained in section 3.

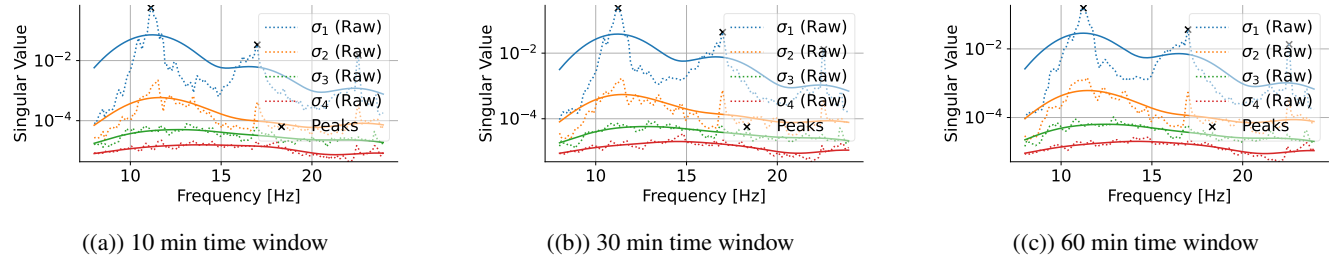


Figure 2.2. Singular Value Decomposition (SVD) of the PSD matrix obtained from the staircase time series data, with different time windows and the parameter `nperseg = 1024`. The plots above are presented on a semi-logarithmic scale.

The corresponding mode shapes (in acceleration unit) are given in Table 2.1.

	Stair 1 X	Stair 1 Y	Stair 1 Z	Stair 2 Z
$f_1 = 11.23 \text{ Hz}$	0.025	0.99	0.11	0.04
$f_2 = 16.99 \text{ Hz}$	0.45	0.09	0.76	0.43
$f_3 = 22.55 \text{ Hz}$	0.23	0.21	0.86	0.38

Table 2.1. Mode shape components (acceleration units) for the different detected mode frequencies.

2. Coherence Analysis [2]

Before developing the peak-picking technique, let's describe another analysis, namely coherence analysis, which will be used in parallel with the PSD analysis to detect the peaks and thus the modal frequencies.

The coherence function, like the PSD matrix, is used to describe the strength of the association between two time series. Its values range from 0 to 1, where a value close to 1 indicates a stronger dependence between the time series. As discussed in this section, the coherence function is particularly useful for identifying modal frequencies in dynamic structural systems, such as the staircase at Livraria Lello. Additionally, as presented in [2], this method aims to reduce the risk of detecting false peaks in Frequency Domain Decomposition, thereby improving the accuracy of modal frequency identification.

2.1. Mathematical Definition of the Coherence Function

The coherence function $\gamma_{ij}(f)$ of two response measurements signals $x_i(t)$ and $x_j(t)$ is defined as :

$$\gamma_{ij}(f) = \frac{|S_{ij}(f)|^2}{S_{ii}(f)S_{jj}(f)} \quad (2.3)$$

Where $S_{ij}(f)$ is defined in 2.1.

Then the coherence matrix is obtained by merging the coherence function so that :

$$\Gamma(f) = \begin{bmatrix} 1 & \gamma_{12}(f) & \cdots & \gamma_{1n}(f) \\ \gamma_{21}(f) & 1 & \cdots & \gamma_{2n}(f) \\ \vdots & \vdots & \ddots & \vdots \\ \gamma_{n1}(f) & \gamma_{n2}(f) & \cdots & 1 \end{bmatrix}$$

Where n is the number of sensors.

2.2. Mathematical Definition of the 3 Peack Picking (PP) indices

As described in [2], the PP indices allow to combine the informations from n sensors into a single function which is suitable for the identification of the natural frequencies.

. 1ST PP INDEX P_1

$$P_1(f) = \sum_{i=1}^n \sum_{j=i+1}^n \left| \frac{1}{\log(\gamma_{ij}(f))} \right|$$

. 2ND PP INDEX P_2

$$P_2(f) = \left| \frac{1}{\log(\sigma_1(f)/n)} \right|$$

. 3RD PP INDEX P_3

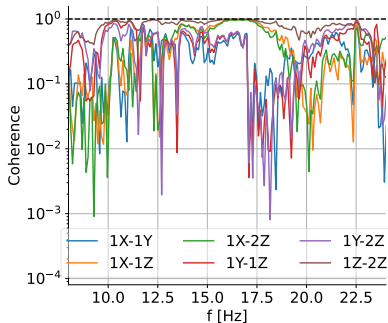
$$P_3(f) = \prod_{k=2}^n \frac{1}{\sigma_k(f)}$$

As explained in [2], the coherence matrix tends to a matrix full of ones at the vibration frequencies, so the first singular value tends to n and all the others tend to 0 at those frequencies. This is emphasized by the fact that the three indices tend to infinity as f approaches one of the vibration frequencies of the structure.

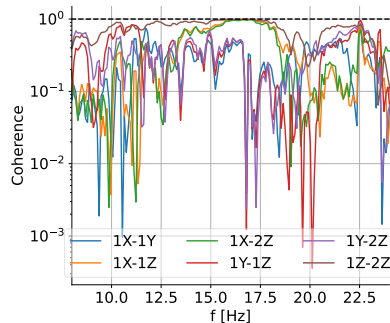
2.3. Results

Figure 2.3 presents the coherence non-diagonal entries obtained from the time series shown in Figure 1.1. The dashed black line indicates a value of 1. It is observed that, in practice, when considering different time window lengths, not all the entries of the coherence matrix tend to 1 at the identified mode frequencies. However, for each of the three mode frequencies (around 11 Hz, 16 Hz, and 22 Hz) identified in Section 1.1, different coherence matrix entries tend to 1. Using the PP indices from the singular values of the coherence matrix should be more readable since the signals are reduced to three.

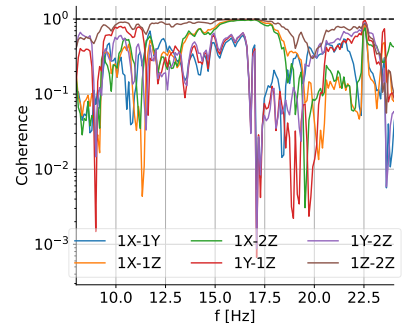
As shown in Figure 2.4, the PP indices peak at the same frequencies identified in Section 1.1, that is at about 11 Hz, 16 Hz, and 22 Hz. However, for the considered time series and the various time windows, it is now observed that the second vibration frequency is the one for which the peak has the maximum value. This result is interesting and reveals that the SVD of the PSD matrix could be used in parallel with the PP indices to develop a method that tracks the evolution of the vibration frequencies over time. The PP indices also reveal that at the frequency of about 11 Hz, there is a sort of double peak. For the time windows of size 30 minutes and 60 minutes, the two neighboring peaks have similar amplitudes, making the peak picking task more difficult.



((a)) 10 min time window



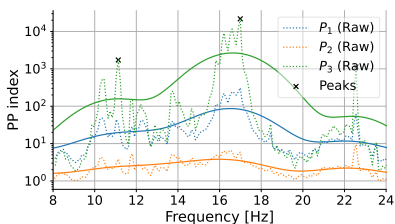
((b)) 30 min time window



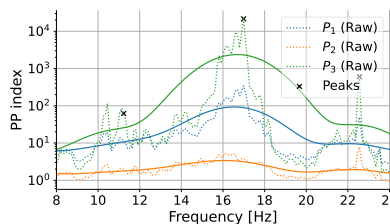
((c)) 60 min time window

Figure 2.3. Coherence indices from the staircase time series data, with different time windows and the parameter $nperseg = 1024$. The plots above are presented on a semi-logarithmic scale.

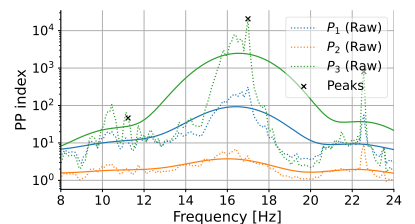
Among the three PP indices, P_3 is the one that has the highest amplitude.



((a)) 10 min time window



((b)) 30 min time window



((c)) 60 min time window

Figure 2.4. PP indices from the staircase time series data, with different time windows and the parameter $nperseg = 1024$. The plots above are presented on a semi-logarithmic scale.

3. Peak-Picking (PP) Method

The peak-picking methods described here are based on the singular values of the PSD matrix, four in our case (since there are four time series data), and the PP indices, of which three were defined from the coherence matrix. For the sake of simplicity, the methods were first applied to one of the seven indices over time and then might be extended to all seven indices.

3.1. Method 1

The principle of the first method is to smooth the singular values of the PSD matrix and the PP indices, which are both functions of frequency, with a Gaussian filter characterized by the parameter σ (the standard deviation of the Gaussian kernel; higher values of σ result in more smoothing)¹.

The steps are as follows :

- 1. Smoothing:** Apply a Gaussian filter to smooth the singular values of the PSD matrix and the PP indices. This helps to reduce noise and detect the bells around the modal frequencies.
- As seen in Figures 2.2 and 2.4, the solid lines indicate the obtained smooth curves with $\sigma = 8$, and the black crosses mark the detected peaks. The curves for the different singular values have the same shape, with the peaks appearing at the same frequencies. Similarly, for the PP indices, the curves follow the same pattern.

¹Gaussian smoothing is a technique used to reduce noise and detail by averaging data points in a way that gives more weight to points closer to the target. For more details, see https://en.wikipedia.org/wiki/Gaussian_filter

Therefore, the method is applied only to the first singular value and the third PP index, as these exhibit the most pronounced peaks, as can be visually confirmed in Figures 2.2 and 2.4.

This first method is applied globally to the entire frequency domain to detect the modal frequencies without using the mode shapes associated with each detected modal frequency.

Moreover, the research domain is defined by the band [8, 24] Hz in this case.

. SENSITIVITY ANALYSIS FOR σ AND nPERSEG

In this section, the influence of the hyperparameters $nperseg$ and σ on the results of Method 1 is studied.

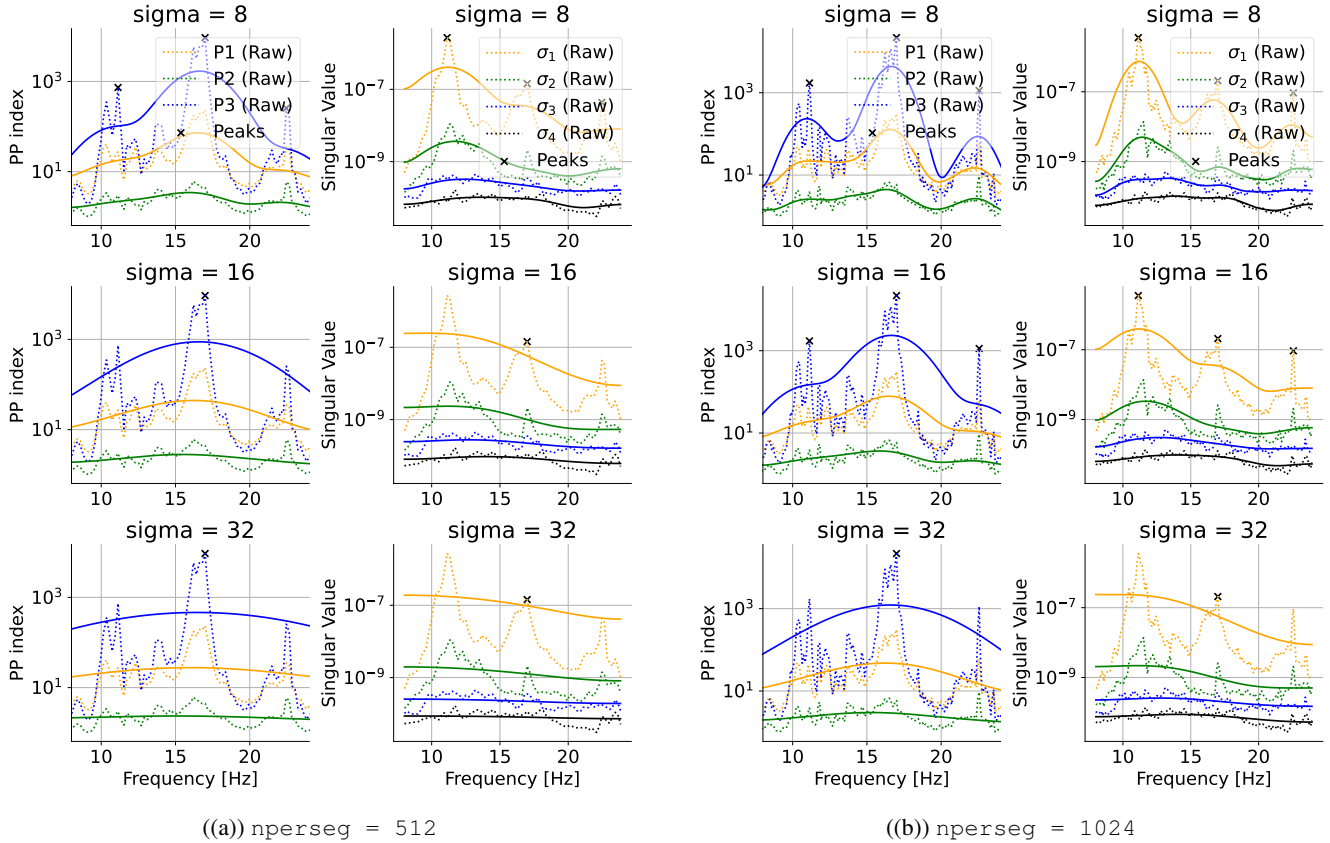


Figure 2.5. PP indices and singular values of the PSD matrix for different values of the parameters σ and $nperseg$. The plots above are presented on a semi-logarithmic scale.

Figure 2.5 shows that the parameter $\sigma = 8$ is the most robust regarding variations of $nperseg$. In fact, with this value, the 3 peaks are always detected for both $nperseg = 512$ and $nperseg = 1024$. Their smoothed curves show 3 bells on either the PP indices or the singular value of the PSD matrix. Moreover, it is observed that the singular values of the PSD matrix tend to show one major peak at the frequencies around 11 Hz, which might help to avoid mismatching between the closely present peaks in the PP indices plot.

3.2. Method 2

The objective of developing the Method 2 is to create an unsupervised approach that does not require an initial estimate of the modal frequency ranges, while also enhancing robustness. This is accomplished by quantifying the similarity between mode shapes using the Modal Assurance Criterion (MAC) index (see Definition 3.1).

Definition 3.1. The Modal Assurance Criterion (MAC) index is a measure used to quantify the similarity between two mode shapes. Given two mode shapes represented by vectors ϕ_1 and ϕ_2 , the MAC index is

defined as:

$$\text{MAC}(\phi_1, \phi_2) = \frac{|\phi_1^H \phi_2|^2}{(\phi_1^H \phi_1)(\phi_2^H \phi_2)}$$

where ϕ_1^H and ϕ_2^H denote the Hermitian (conjugate transpose) of the mode shape vectors ϕ_1 and ϕ_2 , respectively. The MAC index ranges from 0 to 1, where a value close to 1 indicates high similarity between the two mode shapes, and a value close to 0 indicates low similarity.

The MAC index is used to detect frequency sub-domains corresponding to similar modes. For example, Figure 2.6(a) illustrates that for the considered data, there are three main modes, highlighted by yellow squares.

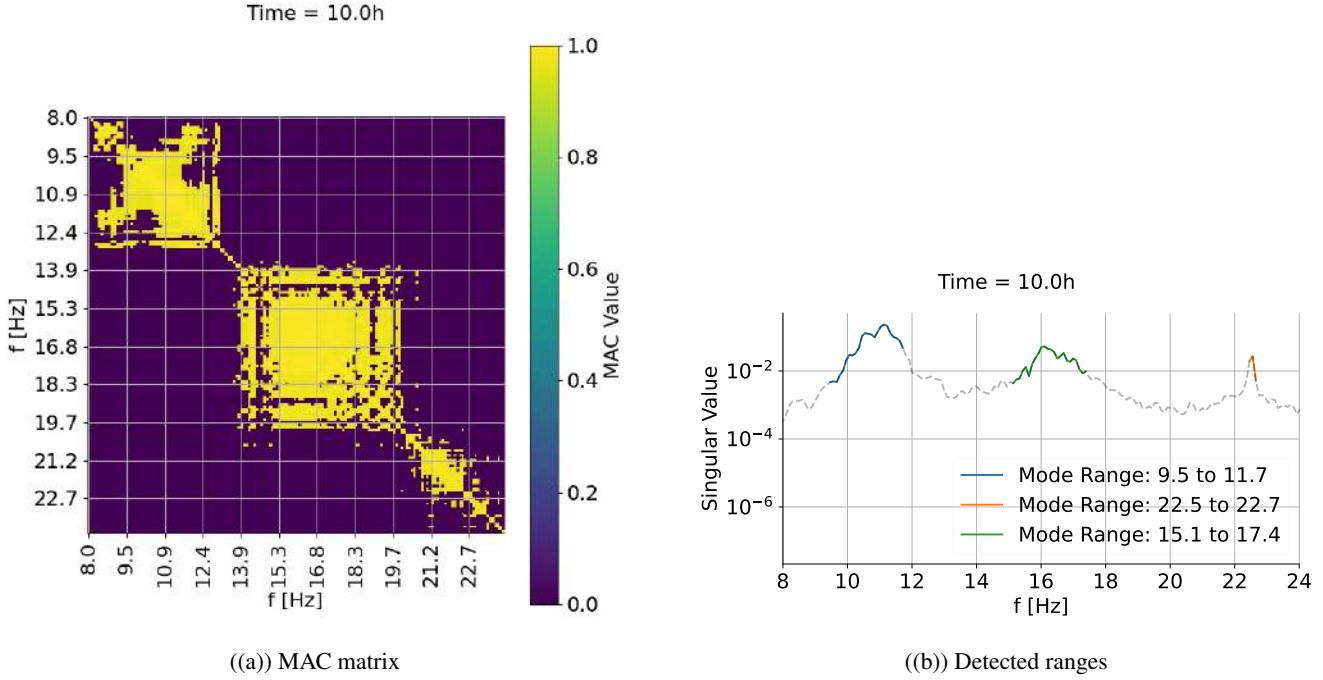


Figure 2.6. Results of Method 2 after processing 10 hours of data when processing multiple files (Section 4) with the same hyperparameters as in Figure 2.7(b). A threshold of 0.95 is applied to the MAC matrix.

The steps of the method are as follows:

- (a) **Frequency Range Detection:** Evaluate the MAC matrix at equally spaced frequencies within a specified frequency band. Apply a threshold to the MAC values to identify ranges of frequencies that correspond to similar mode shapes. The ranges are selected to be contiguous. For example, given four frequencies f_1 , f_2 , f_3 , and f_4 , if $\text{MAC}_{1,2} < \text{MAC}_{\text{threshold}}$ and $\text{MAC}_{1,4} < \text{MAC}_{\text{threshold}}$ but $\text{MAC}_{1,3} > \text{MAC}_{\text{threshold}}$, then the range is defined as $[f_1, f_2]$, and f_4 is excluded (Figure 2.6(a)).
- (b) **Mode Grouping:** Group the detected frequency ranges into modes. Each mode is defined as a contiguous range of frequencies where the MAC values exceed the threshold, indicating similar mode shapes. This grouping helps in identifying distinct modes present in the data (Figure 2.6(b)).
- (c) **Range Evaluation:** Score and select the frequency ranges based on their significance in the context of previously detected modes. This involves comparing the detected frequency ranges with the last n_{mem} identified frequencies to ensure continuity and relevance of the detected modes. n_{mem} is chosen to be equal to 4.

(d) **Peak Picking:** Within the selected ranges, identify the peak frequencies by locating the local maxima.

This step ensures that the most prominent features in the frequency domain are captured as the modal frequencies.

This method is applied to the singular values of the PSD matrix, with a rolling time window and 50% overlap.

4. Processing Multiple Files

Now that the Operational Modal Analysis (OMA) methods have been defined, let's apply them to multiple time series files to analyze the tracking of modal frequencies over time. As a validation technique, the Python package *PyOMA* [3] with the "EFDD" method is used.

4.1. Sensitivity Analysis with `nperseg = 1024`

Figures 2.7 and 2.8 present the results for the morning data, capturing the natural oscillation of the staircase, and for the entire day, where random input excitation is introduced by people walking in the library. Overall, the methods perform better when the library is closed, with no external random excitations. A notable observation in Figure 2.8 is the increased noise in the 22 Hz mode after 5 hours of recording, which can be attributed to the near disappearance of the corresponding peak in the singular values of the PSD matrices, as shown in Figure 2.9(b).

Additionally, Figure A.1 in Appendix A provides a clearer insight into the decrease in modal response during Livraria Lello's opening hours, which corresponds to the observations in Figure 2.8(a). The peak at 17Hz becomes smoother and shifts to around 16Hz, before reverting to its ambient behavior after 19:00.

Focusing on the 5 AM data (Figure 2.7), it is evident that increasing the time window to 30 minutes reduces oscillations for both Method 1 and Method 2. For the modal frequencies at 11 Hz and 16 Hz, the results from Method 1 and Method 2 align closely with those from the *PyOMA* method, but with fewer oscillations. For the 22 Hz modal frequency, both Method 1 and Method 2 show minimal oscillations in their PSDs.

Based on this initial comparison, a 30-minute time window yields more stable results for the 5 AM data using either Method 1 or Method 2.

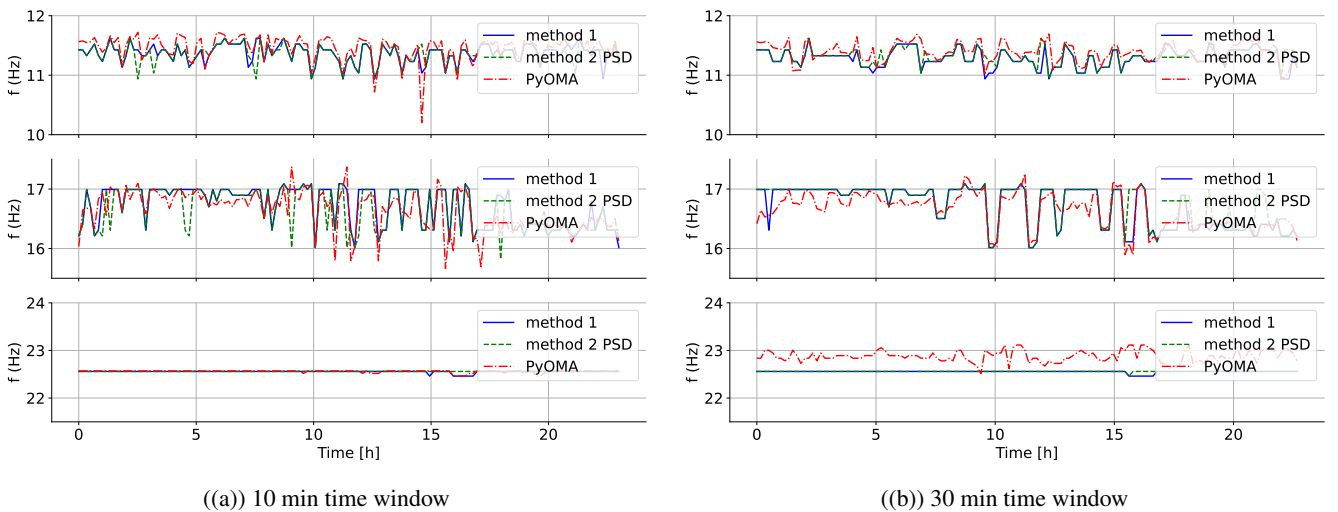
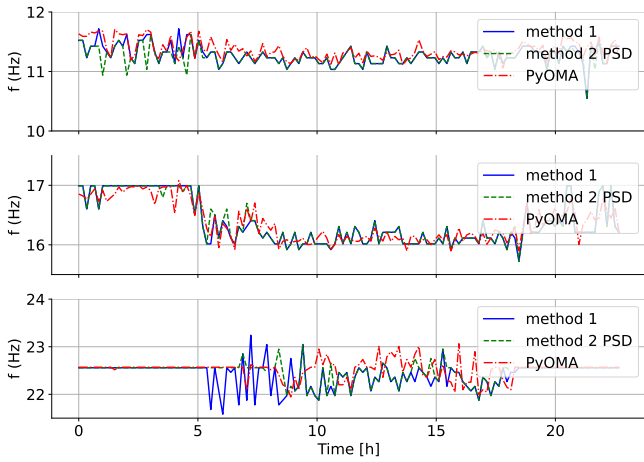
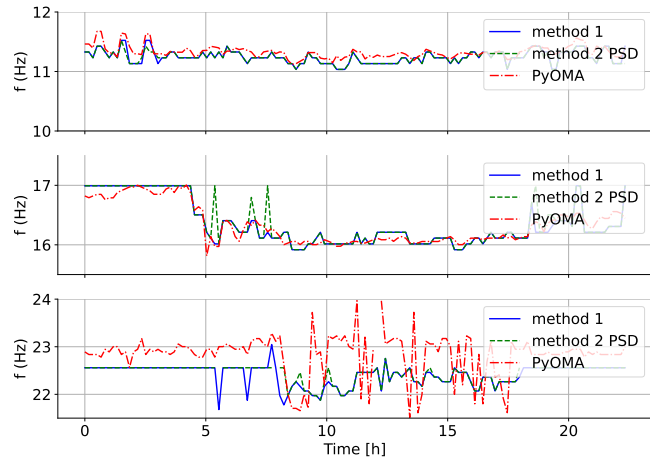


Figure 2.7. Comparison of results from different methods using data collected between 5 AM and 6 AM from July 2, 2023 to July 26, 2023, with various time windows and `nperseg = 1024`. The daily data are concatenated and processed as if it were a continuous time series.

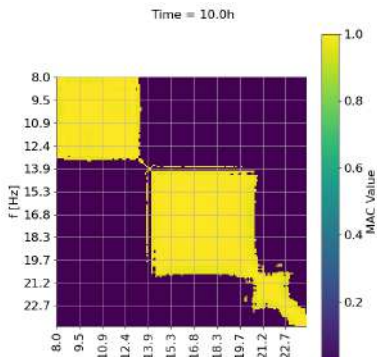


((a)) 10 min time window

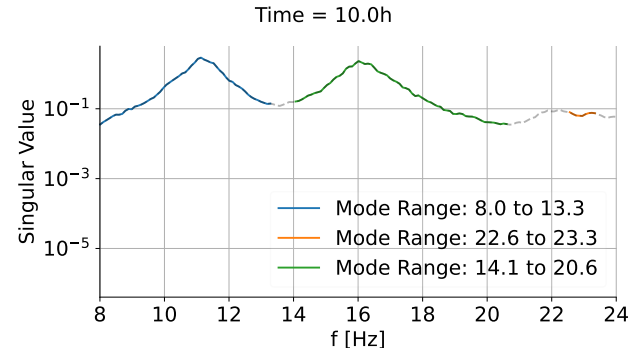


((b)) 30 min time window

Figure 2.8. Comparison of results from different methods using data collected throughout the entire day on July 10, 2023, with various time windows and $n_{perseg} = 1024$.



((a)) MAC matrix

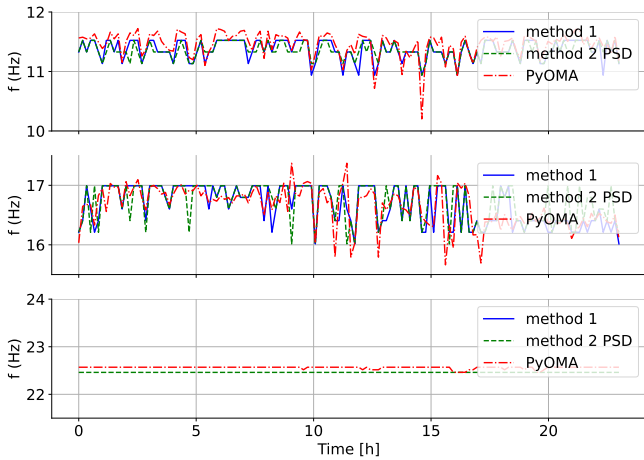


((b)) Detected ranges

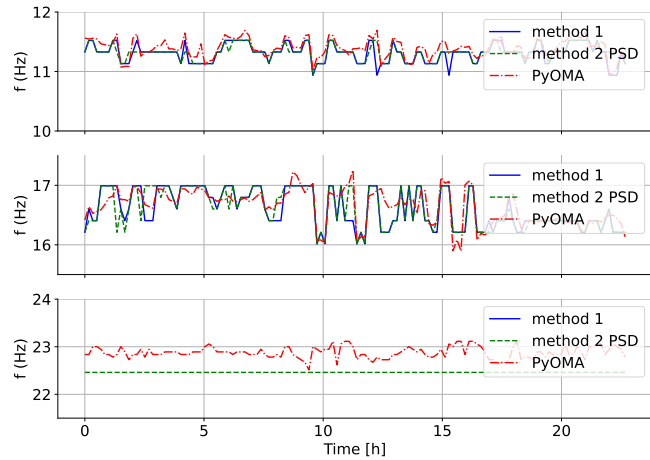
Figure 2.9. Results of Method 2 after processing 10 hours of data when processing multiple files (Section 4) with the same hyperparameters as in Figure 2.8(b). A threshold of 0.95 is applied to the MAC matrix.

4.2. Sensitivity Analysis with $n_{perseg} = 512$

When decreasing n_{perseg} to 512, Method 1 fails to detect the 22 Hz mode because the peak is too sharp. The Gaussian smoothed curve does not capture the corresponding bell with the parameter $\sigma = 8$, as shown in Figure 2.5(a). Therefore, it is better to use $n_{perseg} = 1024$ with Method 1 to avoid excessively sharp bells. Method 2 PSD works well for both n_{perseg} values of 512 and 1024.

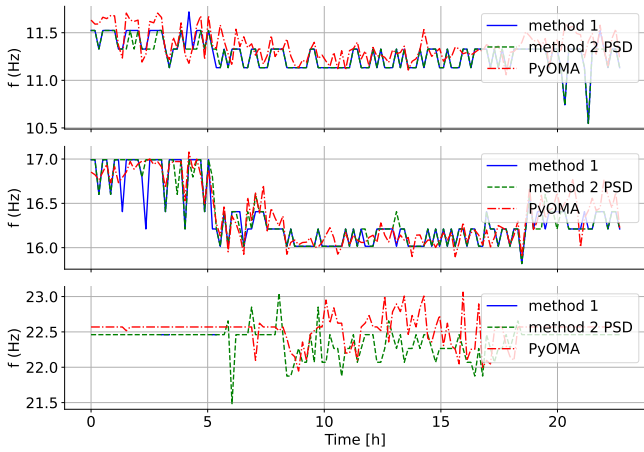


((a)) 10 min time window

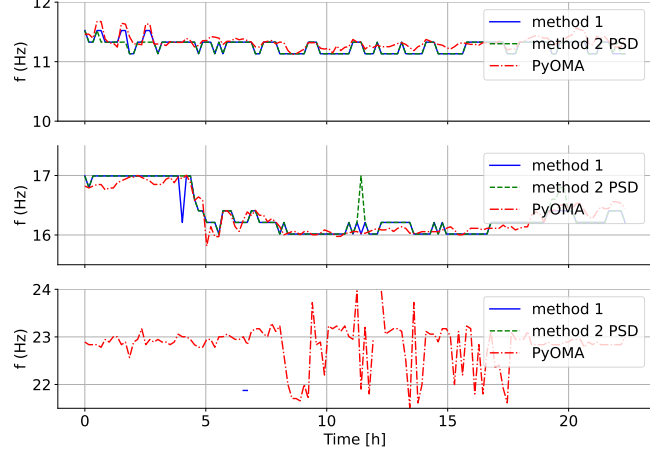


((b)) 30 min time window

Figure 2.10. Comparison of results from different methods using data collected between 5 AM and 6 AM from July 2, 2023 to July 26, 2023, with various time windows and $n_{perseg} = 512$. The daily data are concatenated and processed as if it were a continuous time series.



((a)) 10 min time window



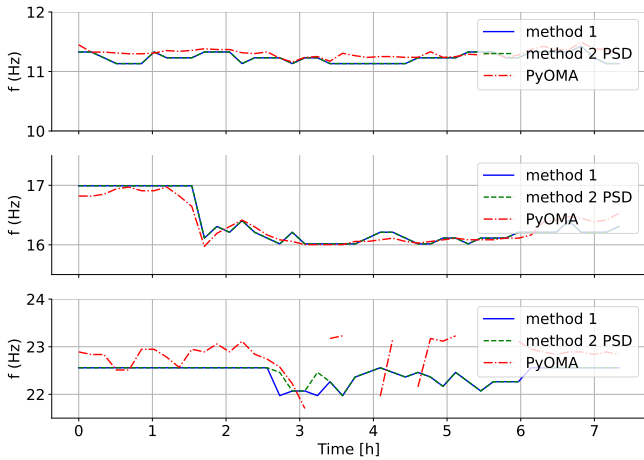
((b)) 30 min time window

Figure 2.11. Comparison of results from different methods using data collected throughout the entire day on July 10, 2023, with various time windows and $n_{perseg} = 512$.

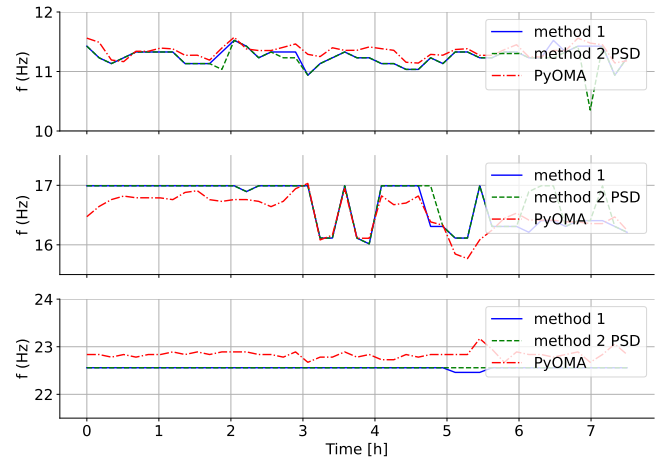
4.3. Results with a 60 min time window

As it was observed that increasing the length of the time window from 10 minutes to 30 minutes reduces oscillations, let's analyze if further extending it to 60 minutes will attenuate the oscillations even more. For this analysis, n_{perseg} is set to 1024 and σ to 8, as discussed above.

Figure 2.12 shows the results for both daily and morning data with this extended time window. It is confirmed that the detected frequencies exhibit fewer oscillations with both methods. Additionally, with the daily data (Figure 2.12(a)), the PyOMA EFDD method fails to accurately track the 22 Hz mode during the opening hours of the Livraria.



((a)) daily data



((b)) 5 AM data

Figure 2.12. Results from different methods using data collected throughout the entire day on July 10, 2023 (2.12(a)) and between 5 AM and 6 AM from July 2, 2023 to July 26, 2023 (2.12(b)), with $n_{perseg} = 1024$.

Chapter 3

Data Collection on "Alfredo" 2-Story Experimental Structure

The experimental structure is a 2-story structure where the stiffness and masses of each floor can be modified by adding/removing reinforcement bars or adding/removing masses. The goal of this experiment is to collect 10-minute time series data from different configurations of the "Alfredo" structure, which will then be concatenated to obtain a longer time series containing occurrences of damage. Damage is defined as either a decrease in stiffness or mass.

The nomenclature for the signal naming is $M_i_j_k$, where:

- i indicates the test number. One test corresponds to either a change in mass or stiffness. For each type of change (mass or stiffness), a test with high variations and another test with low variations will be performed.
- j indicates the variant for a given test. Variants represent the same kind of damage level but with different configurations. Since the structure is not symmetrical, there are multiple configurations for each test.
- k indicates the step of a given test with a specific configuration. The different configurations will have common steps.

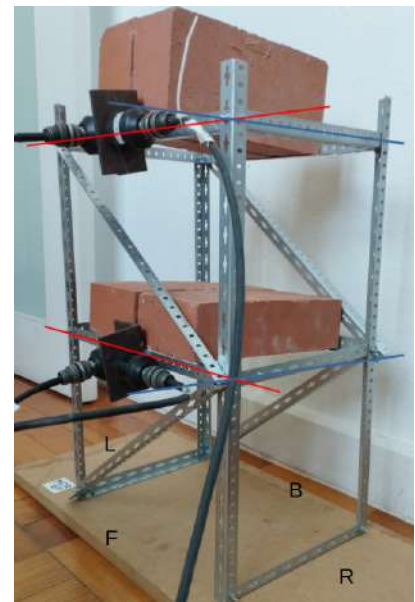


Figure 3.1. M_0_0_0, the red axis represents the x-direction, and the blue axis represents the y-direction. Letters F, B, L and R indicates Front, Back, Left and Right positions with respect to Alfredo.

The 4 accelerometers allow a representation of the "Alfredo" structure as a 4 Degree of Freedom (DoF) system, with the x-axis and the y-axis represented by the red and the blue axes, respectively, in Figure 3.1. The first floor and the second floor are denoted by the indices 1 and 2 for the x and y axes.

1. Test $i = 0$

For the first test, the damages are simulated by variations in the bracing of the reference structure M_0_0_0. These variations are considered significant and should therefore be easier to detect numerically. Table 3.1 shows the different configurations by indicating the number of braces present on each floor. The braces are only added to the faces with the longer sides (x-axis). The Figures B.1 and B.3 in Appendix B show the different configurations and the obtained accelerograms for the first test.

	Variant 0	1st floor	2nd floor	Variant 1	1st floor	2nd floor
Step 0	M_0_0_0	2 bars	2 bars			
Step 1	M_0_0_1	2 bars	0 bars	M_0_1_1	0 bars	2 bars
Step 2	M_0_0_2	1 bar	0 bars	M_0_1_2	0 bars	1 bar

Table 3.1. First test: Bracing variations.

2. Test $i = 1$

The second test consists of varying the stiffness of the stories less significantly than in the first test. Instead of removing bracings, the four columns of the structure are doubled (two beams next to each other instead of one). In each step, the doubling is removed progressively. Table 3.2 contains descriptions of the configurations for each step of each variant. For describing the column positions, "F" stands for "Front," "B" for "Back," "L" for "Left," and "R" for "Right" (see Figure 3.1). The Figures B.4 and B.5 in Appendix B show the different configurations and the obtained accelerograms for the second test.

	Variant 0	FL	FR	BL	BR	Variant 1	FL	FR	BL	BR
Step 0	M_1_0_0	double	double	double	double					
Step 1	M_1_0_1	double	double	double	simple					
Step 2	M_1_0_2	double	simple	double	simple	M_1_1_2	double	double	simple	simple
Step 3	M_1_0_3	double	simple	simple	simple					

Table 3.2. Second test: Column stiffness variations.

3. Test $i = 1$ bis

The same second test is realised with the masses at both stories doubled, two bricks instead of one. The Figures B.6 in Appendix B show the obtained accelerograms for this test.

4. Test $i = 2$

The third test also involves variations in the bracing of the structure, similar to the second test. However, there are a few differences: the mass of the second floor is increased by one brick (see the configuration in Appendix B.7), and during the experimental process, the bracing was added in such a way that it could be removed without tightening any bolts, thus avoiding unwanted modifications. This test ensures that the tightening of the original structure's bolts does not increase throughout the steps. Table 3.4 describes the different configurations. Appendix B.8 shows the obtained accelerograms for this test.

	Variant 0	1st floor	2nd floor
Step 0	M_2_0_0	2 bars	2 bars
Step 1	M_2_0_1	1 bars	2 bars
Step 2	M_2_0_2	0 bar	2 bars
Step 3	M_2_0_3	0 bar	1 bars
Step 4	M_2_0_4	0 bar	0 bars

Table 3.3. First test: Bracing variations.

5. Test i = 3

The fourth test involves varying the mass on each floor by removing bottles (see the configurations in Appendix B.9). Table 3.4 presents the different configurations. Appendix B.14 shows the obtained accelograms for this test.

	Variant 0	1st floor (# bottles)	2nd floor (# bottles)
Step 0	M_3_0_0	3	3
Step 1	M_3_0_1	2	3
Step 2	M_3_0_2	2	2
Step 3	M_3_0_3	1	2
Step 4	M_3_0_4	1	1
Step 5	M_3_0_5	0	1
Step 6	M_3_0_6	0	0

Table 3.4. Fourth test: Mass variations.

Chapter 4

Part II : Statistical Anomaly Detection for Damage Identification Using Temporal and Frequency Data

The second part of this report presents the results obtained by applying the statistical method for damage detection monitoring, as presented in [4], to a 4-story experimental structure [5] and the staircase of Livraria Lello.

1. Overview of the Method

The method is composed of 3 main steps :

- (a) **Compute the Novelty Index (NI):** Extract Symbolic Data Objects (SDOs) representing the statistical distribution of time and frequency domain information using Time-Frequency IQRM objects. The NI is then computed by evaluating the largest distance between prototypes, determined through k-medoids clustering.
- (b) **Compute the Confidence Boundary (CB):** Establish the CB dynamically within each time-window, based on a t-Student distribution of NI values. This boundary is used to identify when the NI surpasses a critical threshold, indicating a potential structural anomaly.
- (c) **Compute the Detection Index (DI):** Compare the current NI with the calculated CB to obtain the DI. A positive DI indicates the presence of damage or structural novelty.

The figure 4.1 summarizes these steps schematically.

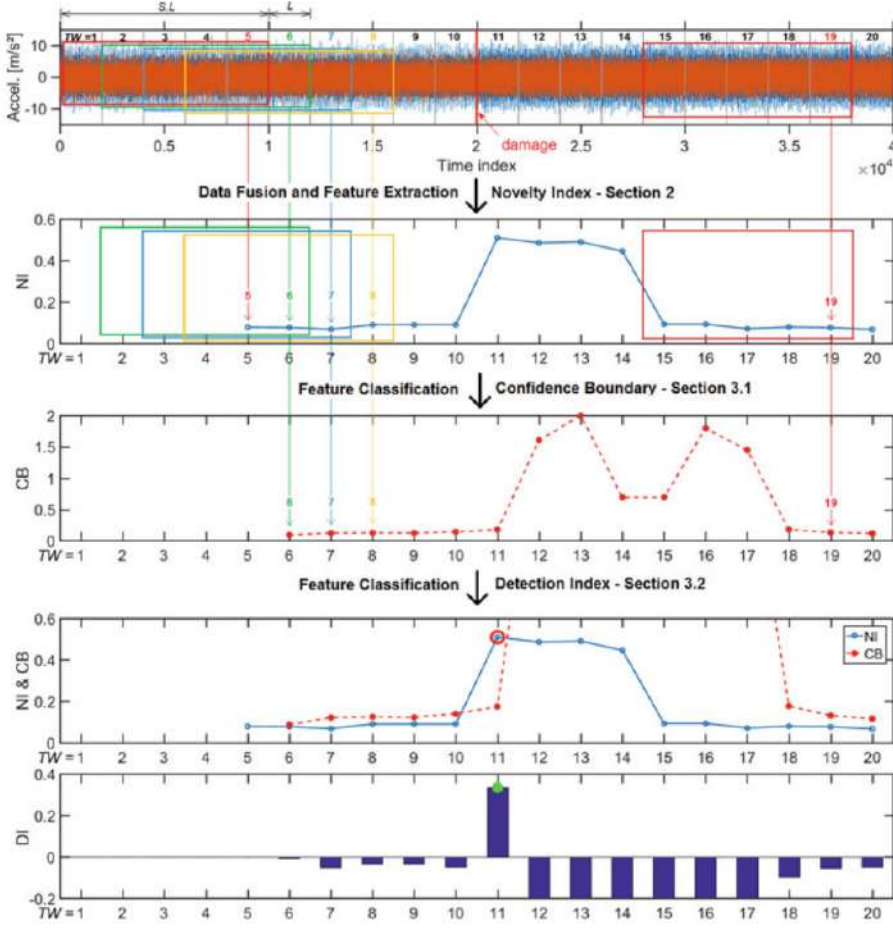


Figure 4.1. Overview of the statistical method presented in [4]. The figure is extracted from [4].

2. Results from the 4-Story Experimental Structure

First, a single iteration of Method 2 (Section 3.2) from Part II (Chapter 2) is applied to the reference time series data (Figure 4.2) to extract the first modal frequency of the structure. To improve the frequency domain analysis, the DC component is removed from the original data.

As shown in Figure 4.3, the first mode occurs at a frequency of $f_1 = 7.42$ Hz. This frequency is then used to estimate the required time window size, $L \cdot S$, necessary to capture the structure's dynamic behavior. The time window size is determined using a simple rule:

$$L \cdot S = \frac{1000}{f_1} = 134.77.$$

To account for $S = 5$ SDOFs per time window, as proposed in [4], a reference time window length of $L_{\text{ref}} = 27$ s is used, leading to a total time window size of

$$S \cdot L_{\text{ref}} = 135 \text{ s.}$$

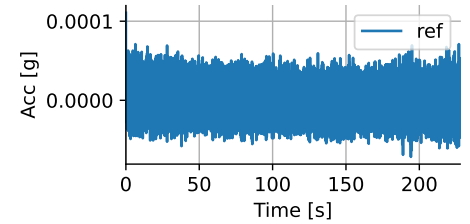


Figure 4.2. Time serie record from the first accelerometer with the undamaged structure (fully braced).

Figure 4.4 shows some of the time series of the damaged structure. To test the behavior of the statistical method, one selected damaged time series is concatenated with the reference time series. The resulting signal

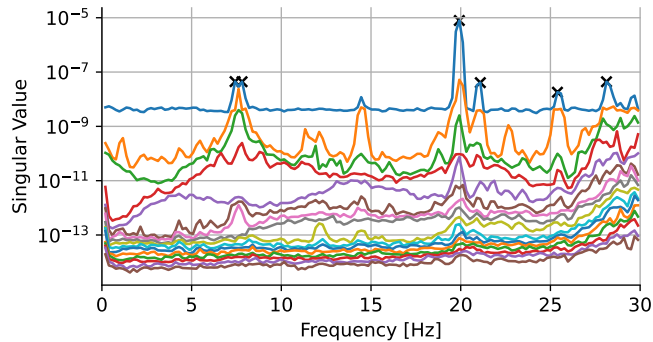


Figure 4.3. Singular value of the SVD of the PSD matrix obtained from the reference time series data of the experimental structure with the parameter $nperseg = 1024$.

is discontinuous. To check whether the method detects the discontinuity or the damage, the second and third thirds of the reference time series are swapped to introduce discontinuities. The time at which the swap occurs is indicated by the grey dashed line, and the time at which the damage occurs is marked by the red dashed line in Figure 4.5.

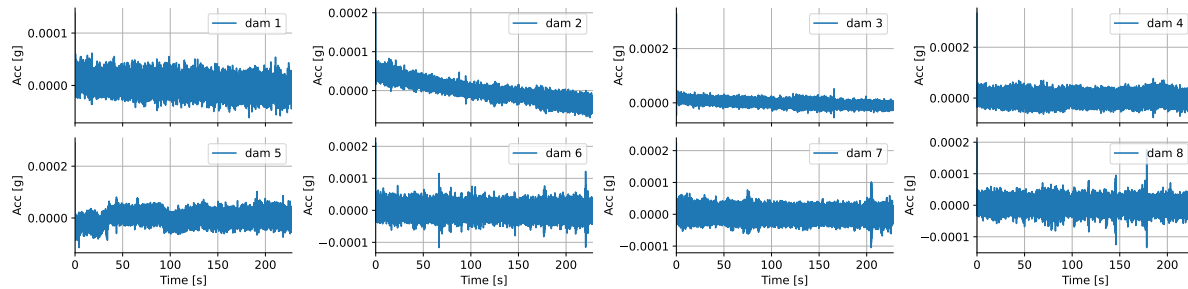
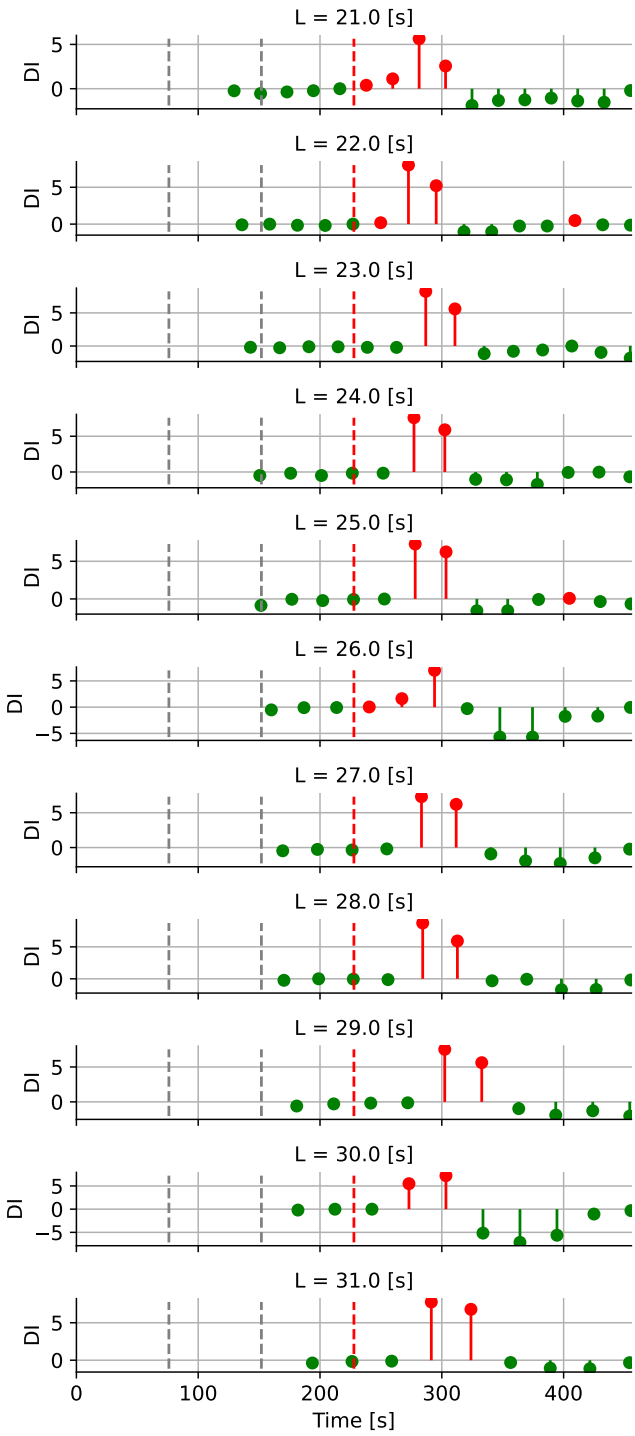
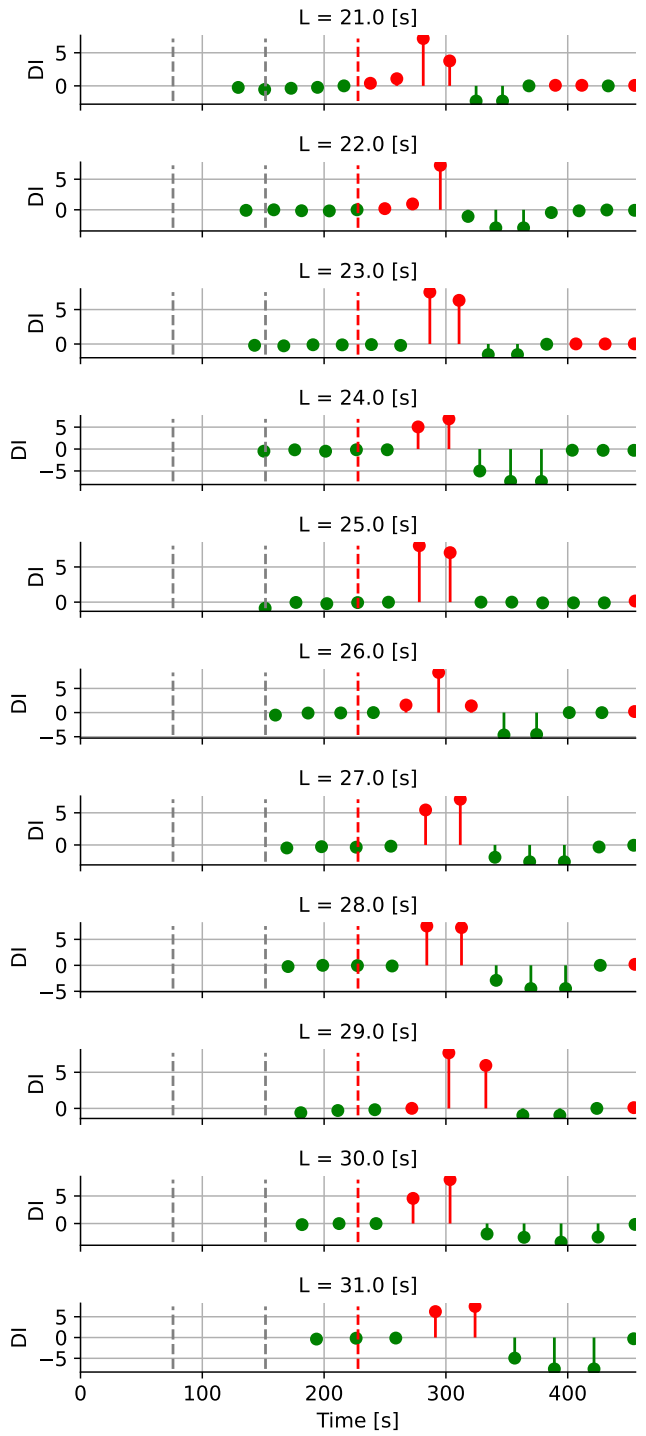


Figure 4.4. Time series records from the first accelerometer with the 8 different damaged structures (see [5] for details about the applied damage).

Figure 4.5 shows the Detection Indexes (DI) obtained for damages 1 and 2 with hyperparameters $S = 5$ and $k = 3$. It is observed that the damages are detected correctly for all the SDO lengths L . To avoid false positives, as suggested in [4], an alarm should be raised only if the DI is positive for more than half of the considered SDO lengths. Applying this principle, with damage 2 applied, one false positive is still detected around 450 s.



((a)) Damage 1 applied



((b)) Damage 2 applied

Figure 4.5. Results from different damages applied using the statistical method on the 4-story experimental structure. The hyperparameters are $k = 3$ (for the clustering) and $S = 5$ SDO's.

3. Results from the "Alfredo" 2-Story Experimental Structure

The data collected from the "Alfredo" structure (Chapter 3) allow for testing the statistical method with increasing levels of damage, thereby assessing the method's robustness in adapting to the structure's changing behavior and detecting successive damages. Refer to the tests described in Chapter 3 for details about each configuration.

3.1. Test $i = 0$

First, applying Method 2 presented in Section 4 to M_0_0 and M_0_1 results in Figures 4.6 and 4.7 respectively, where a decrease in the first two detected modes is observed for M_0_0. However, as shown in the plot of the singular values of the PSD (Figure B.2), this decrease is not easily identifiable visually. Method 2 employs the MAC matrix (`mac_threshold=0.9`) to ensure consistent tracking of the same modes throughout the iterations.

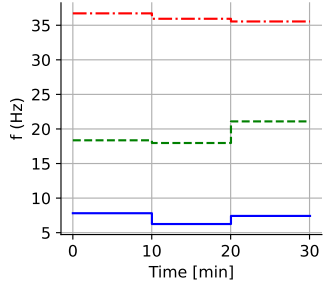


Figure 4.6. Modal frequencies tracked for M_0_0.

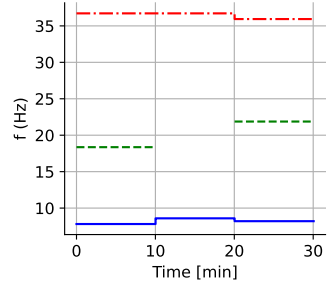
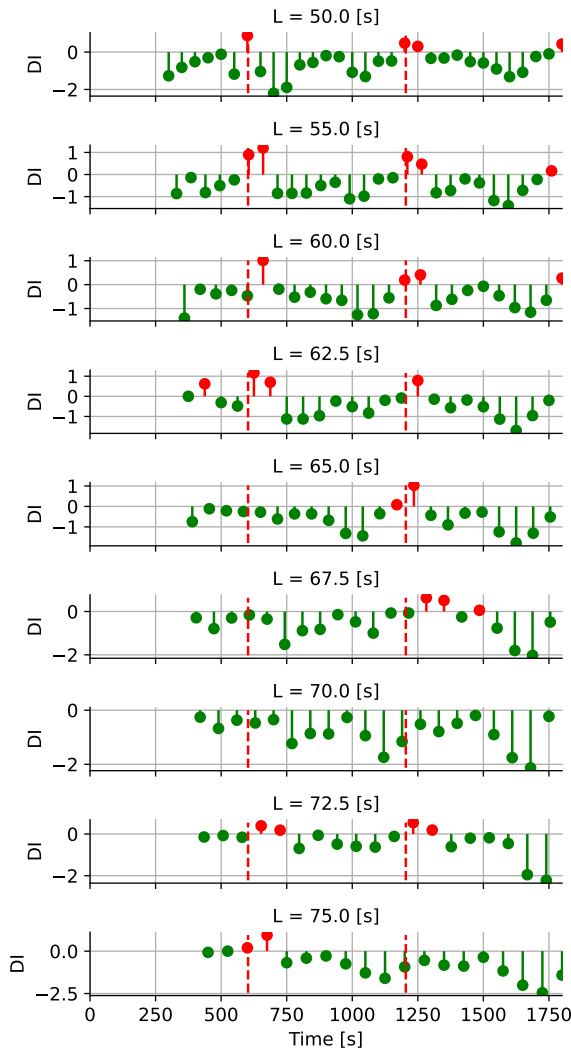
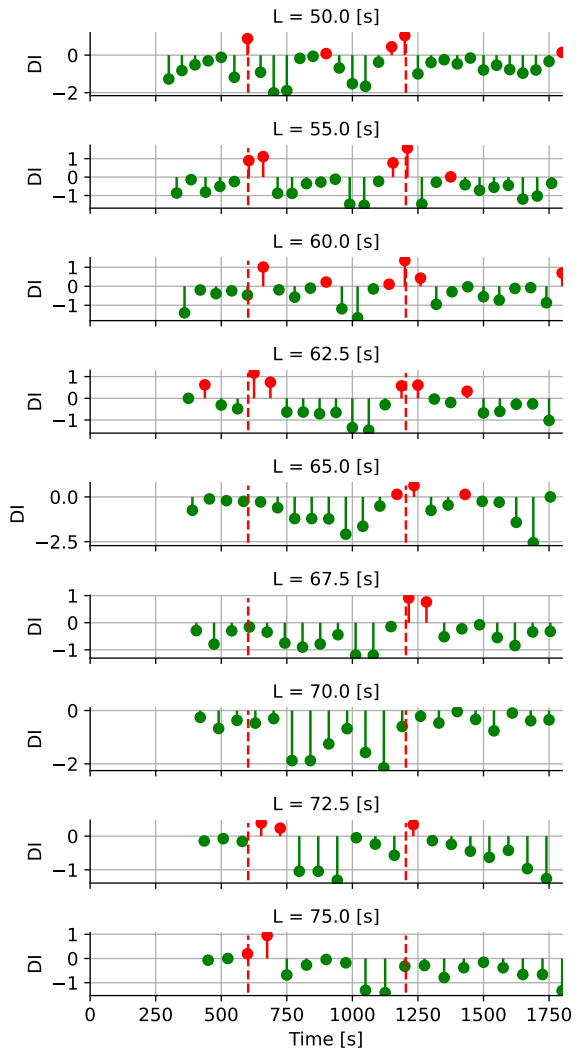


Figure 4.7. Modal frequencies tracked for M_0_1.



((a)) Obtained Detection Index with the variant 0 of the first test.

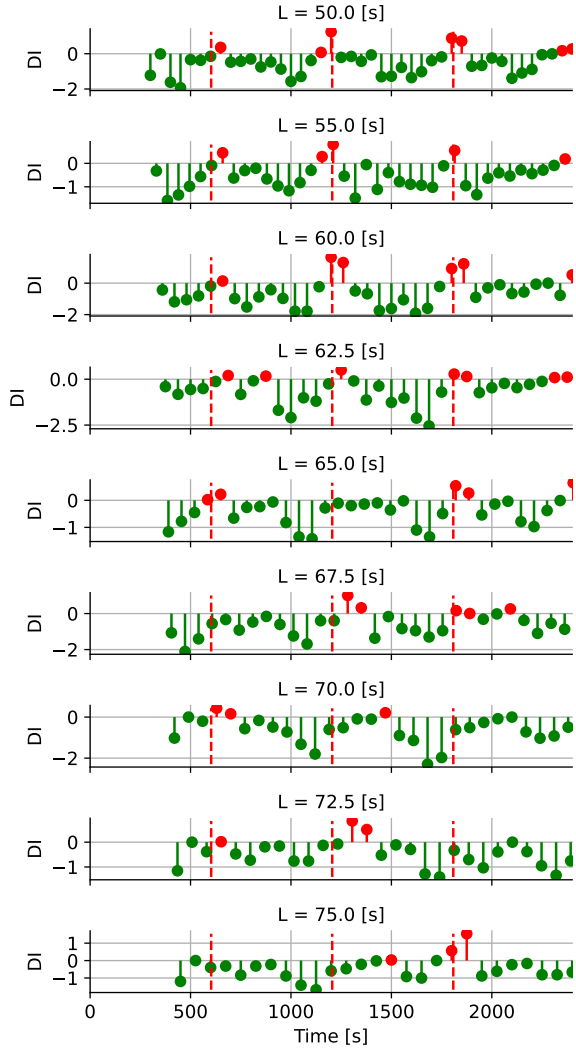


((b)) Obtained Detection Index with the variant 1 of the first test.

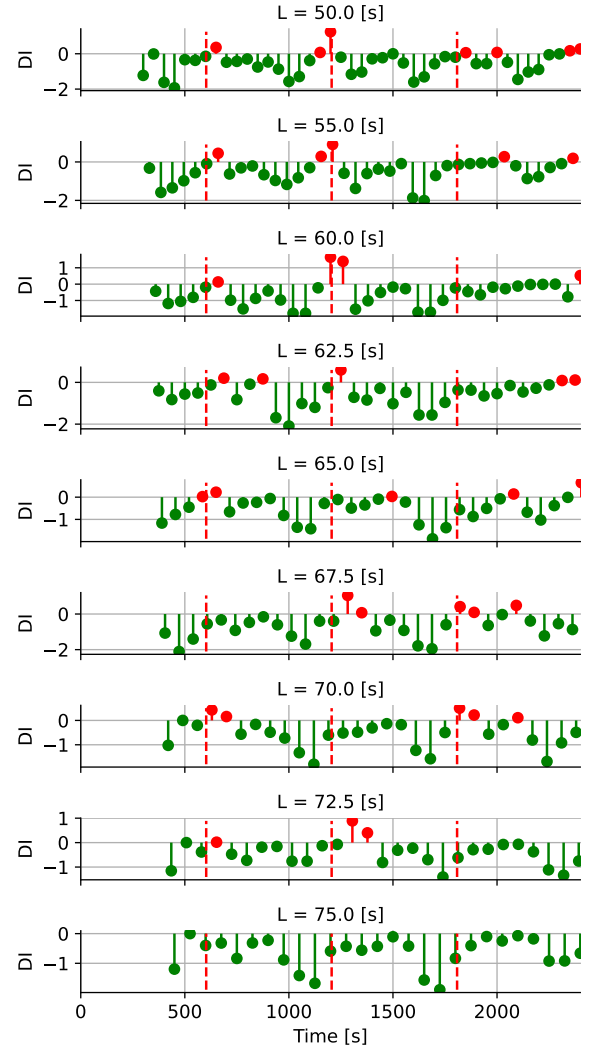
Figure 4.8. Results from different damages ($i = 0$) applied using the statistical method on "Alfredo" 2-Story Experimental Structure. The hyperparameters are $k = 3$ (for the clustering) and $S = 5$ SDO's.

Figure 4.8 illustrates the DI index over time, obtained from the statistical analysis. The results are conclusive, as for the two applied damage cases (indicated by the red dashed lines), the DI index is positive for more than half of the L values. Additionally, no false positives were detected in this case.

3.2. Test $i = 1$



((a)) Obtained Detection Index with the variant 0 of the second test.



((b)) Obtained Detection Index with the variant 1 of the second test.

Figure 4.9. Results from different damages ($i = 1$) applied using the statistical method on "Alfredo" 2-Story Experimental Structure. The hyperparameters are $k = 3$ (for the clustering) and $S = 5$ SDO's.

In this case, Figure 4.9 shows that for configuration 1, the method does not identify the third damage for more than half of the window sizes. This missed detection might be explained by the fact that Test $i = 1$ involves variations in the stiffness of the vertical elements, which are less significant than changes in the bracing configuration.

3.3. Test $i = 1$ bis

Figure 4.10 presents the results, where the damages are correctly identified, and no false positives occur.

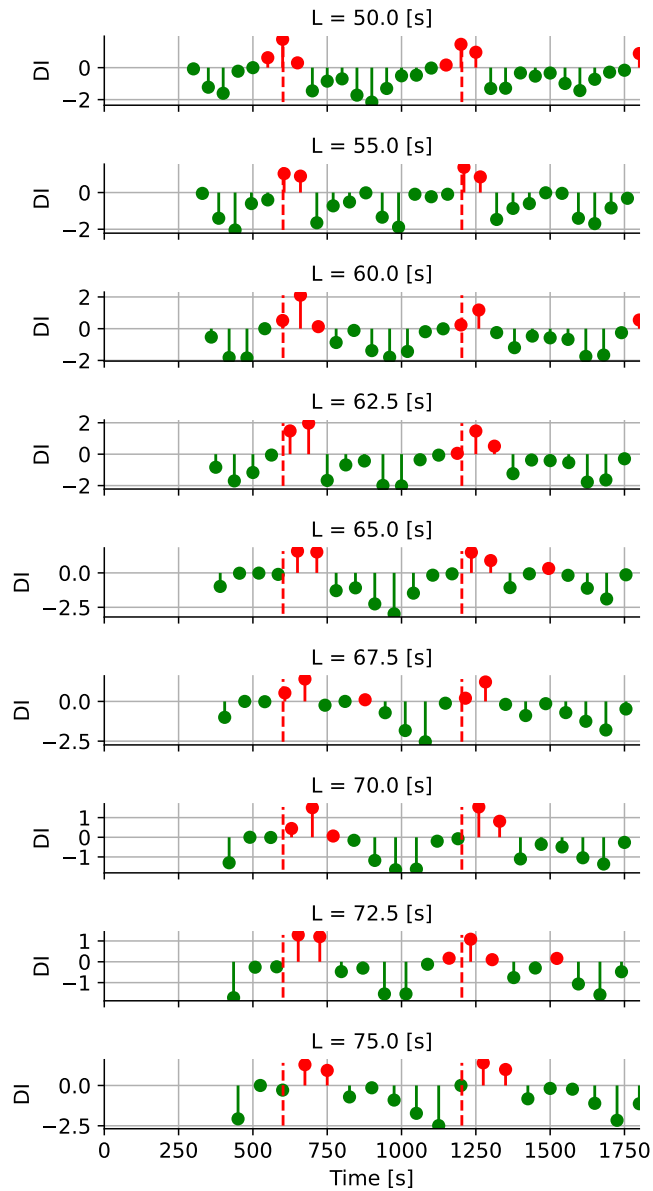


Figure 4.10. Results from different damages ($i = 1 \dots 8$) applied using the statistical method on "Alfredo" 2-Story Experimental Structure. The hyperparameters are $k = 3$ (for the clustering) and $S = 5$ SDO's.

3.4. Test $i = 2$

Figure 4.11 presents the results, where the damages are correctly identified, with only one false positive occurring in the final iterations.

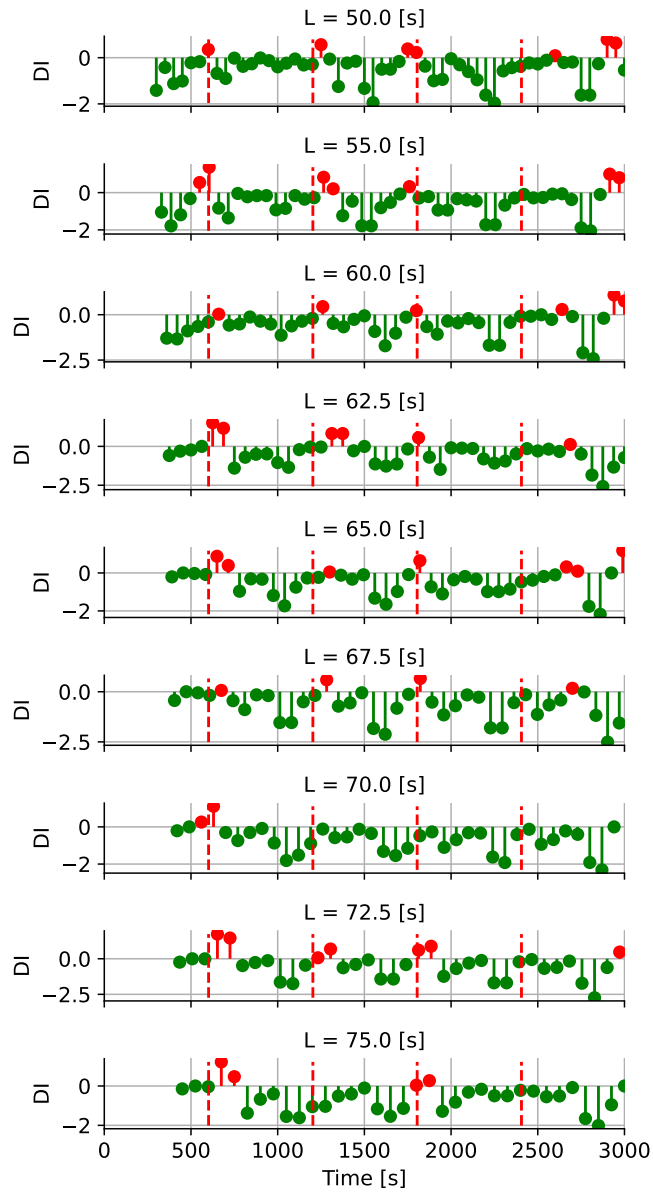
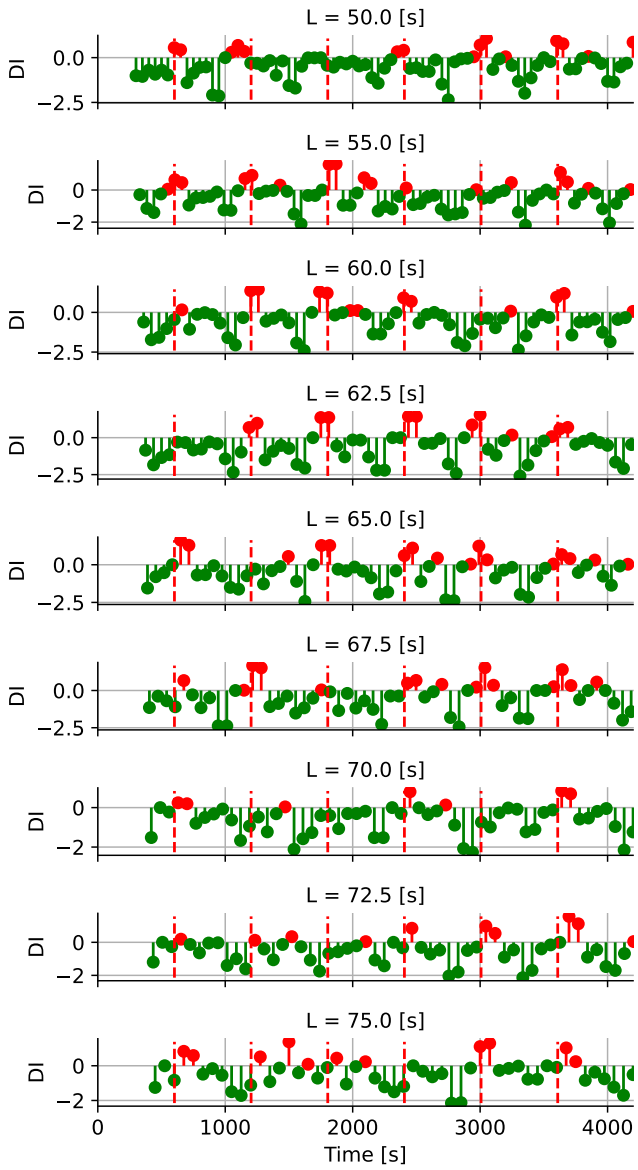


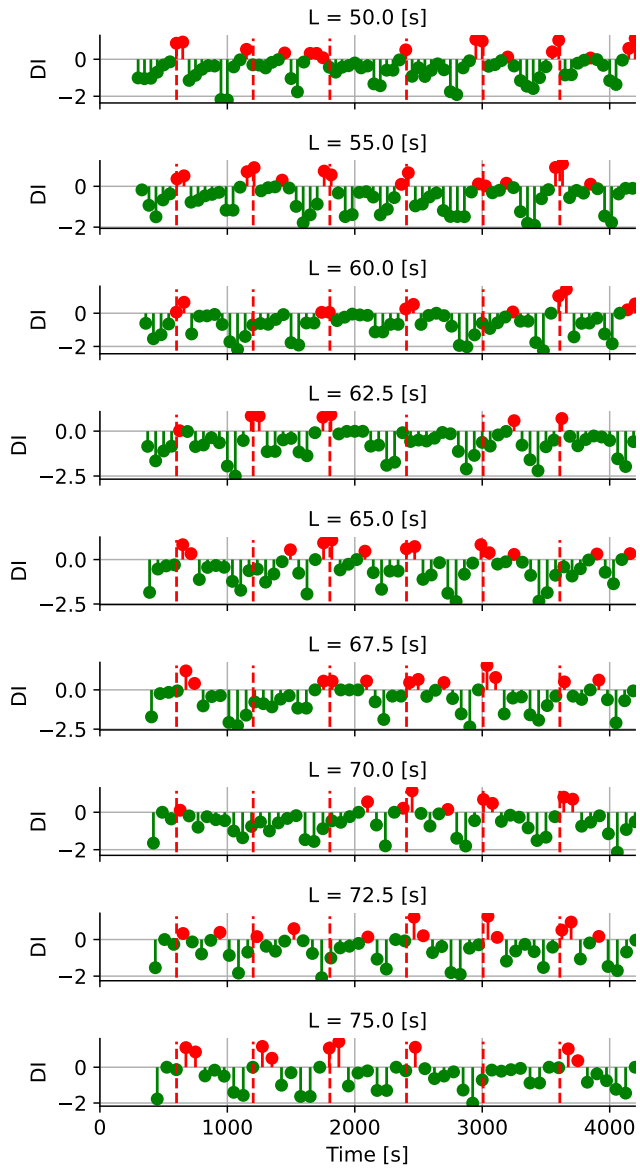
Figure 4.11. Results from different damages ($i = 2$) applied using the statistical method on "Alfredo" 2-Story Experimental Structure. The hyperparameters are $k = 3$ (for the clustering) and $S = 5$ SDO's.

3.5. Test $i = 3$

In this test, Figure 4.12 shows that the damages are correctly identified. The hyperparameters $k=2$ and $k=3$ were used. While varying the number of clusters does not significantly affect the overall results, it does influence the occurrence of false positives.



$k = 2$



$k = 3$

Figure 4.12. Results from different damages ($i = 3$) applied using the statistical method on "Alfredo" 2-Story Experimental Structure. The hyperparameters are $S = 5$ SDO's and k varying (for the clustering).

4. Results from the Livraria Lello Staircase

When applying the statistical method to the night data of the Livraria Lello staircase, as shown in Figure 4.13, the occurrence of false positives varies with the choice of the parameter L . For parameters such as $L = 500$ s, it appears that the false positives are periodic and arise due to the junction of data from night to night. Although a Hamming Window is applied to reduce the effects of these discontinuities, false positives still occur. Therefore, selecting the appropriate value for the parameter L is crucial to minimize false positives in this case.

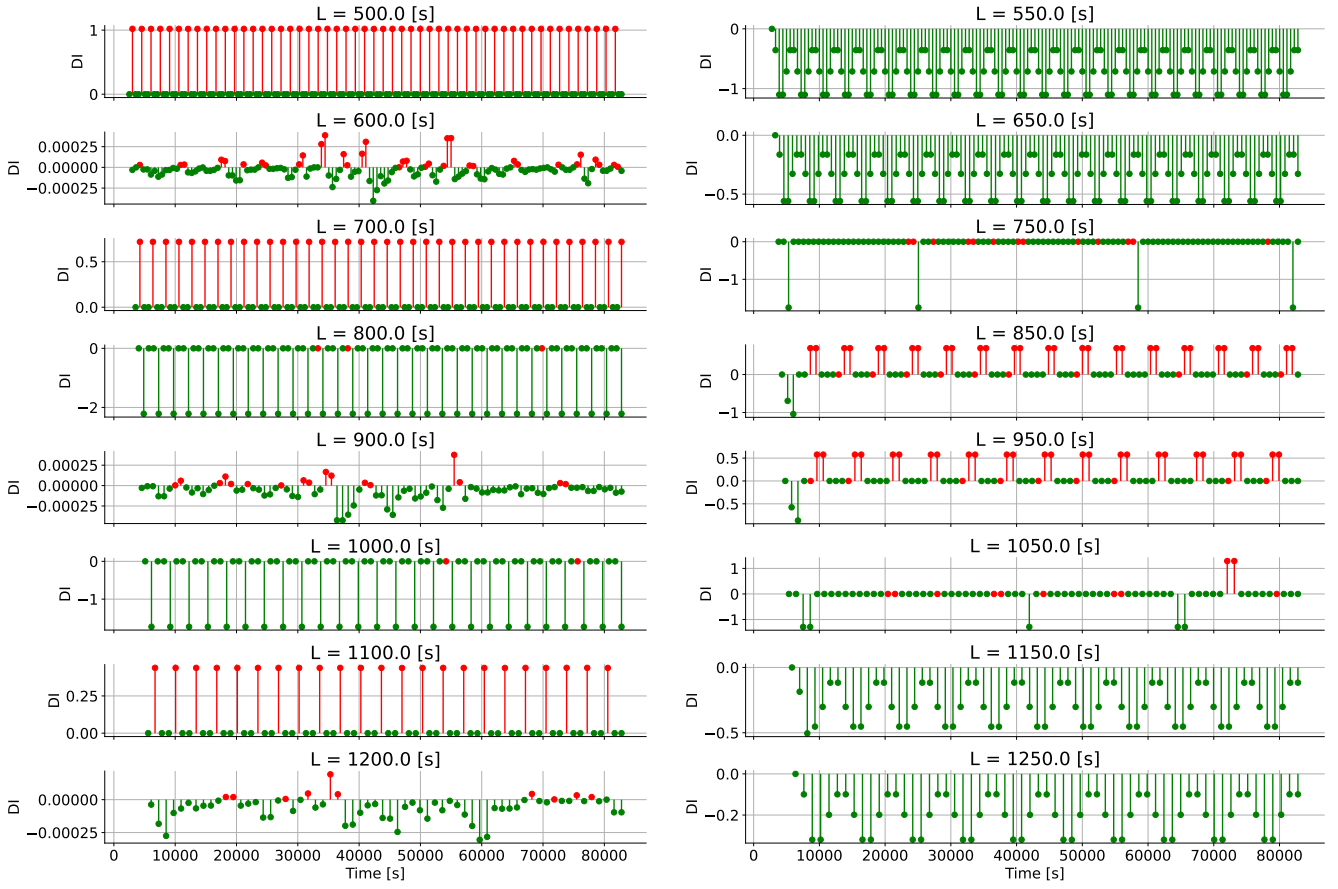


Figure 4.13. Results obtained by applying the statistical method to the Livraria Lello staircase, using the "LelloNight_Jul23_Apr24" data. The hyperparameters are $S = 5$ SDOs and $k = 3$. The night data are concatenated and processed as if they form a continuous time series. Therefore, the time axis is indicative only.

Figure 4.14 shows the results obtained when applying the statistical method to the daily data. Many unexpected false positives occur even after testing several values for the L parameter. However, the highest positive DI values occur at the opening and closing of the library, which is expected since, as seen in Chapter 2, there is a drop in the modal frequencies at those times.

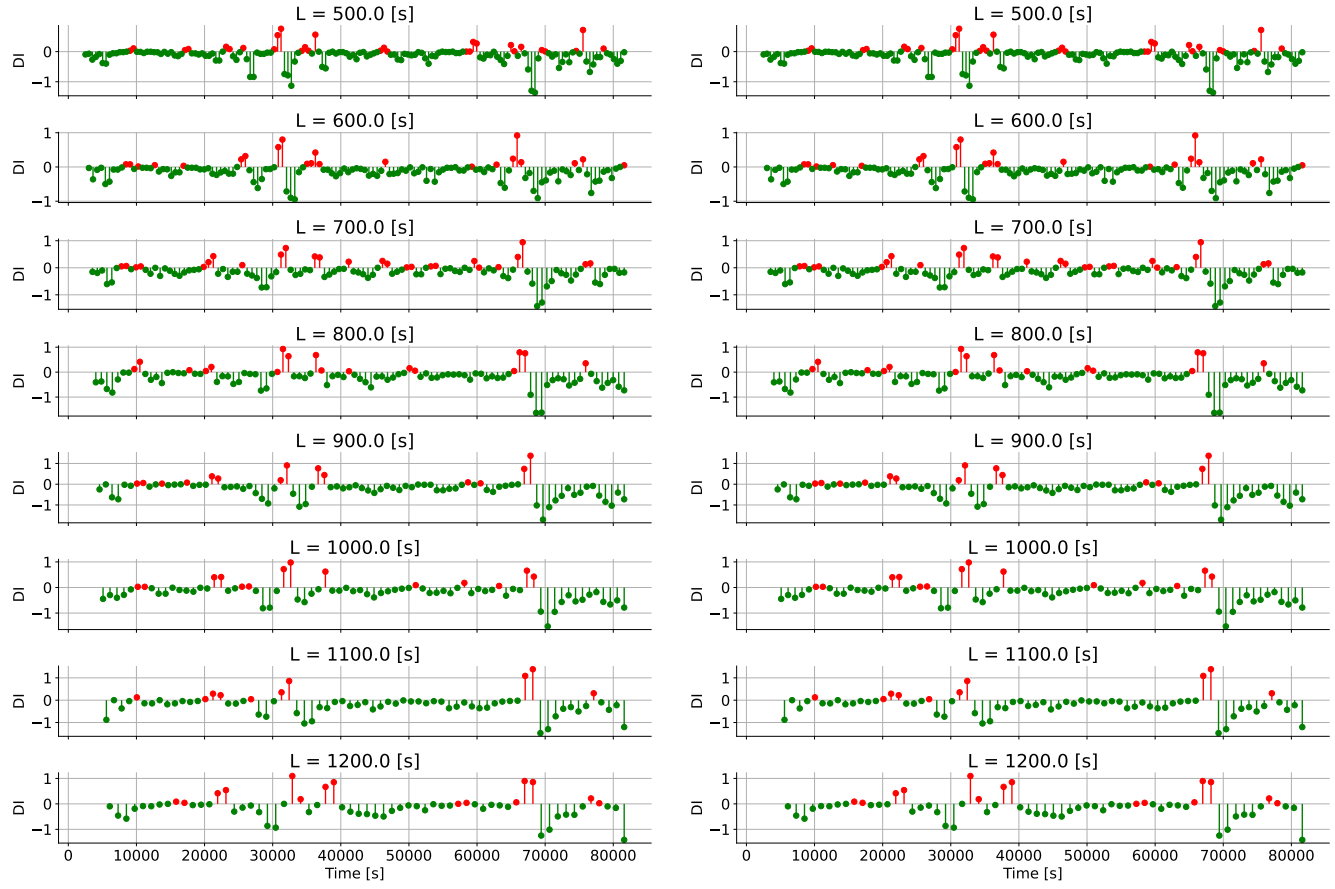


Figure 4.14. Results obtained by applying the statistical method to the Livraria Lello staircase, using the "Lello_2023_07_10_WholeDay" data. The hyperparameters are $S = 5$ SDOs and $k = 3$.

Chapter 5

Conclusion

1. Conclusion

In this report, two Operational Modal Analysis (OMA) methods were developed based on the Power Spectral Density (PSD) matrix obtained using the Welch method. From the PSD matrix, the coherence matrix was computed to derive three Peak Picking indices.

The two OMA methods yielded results consistent with the *PyOMA* "EFDD" method when the hyperparameters were appropriately chosen. These methods are applicable for tracking the natural frequencies of structures over time, provided that the hyperparameters `nperseg`, σ (only for Method 1), and the time window are selected correctly.

The advantage of Method 2 is that it is unsupervised and does not require manually setting the ranges of interest for the modal frequencies. Other hyperparameters, such as the resolution for frequency peak picking, were not discussed in detail. For simplicity, the resolution was set to 1 index, which is the highest resolution. Additionally, the `n_mem` parameter was set to 4 without further investigation. In this study, the expected number of modes was 3 based on visual inspection of the frequency domain results.

A statistical analysis derived from [4] was implemented and validated using data collected on the experimental "Alfredo" structure. The results were conclusive, and applying the method to the Livraria Lello staircase revealed that the choice of the hyperparameter L was crucial to avoid periodic false positives.

2. Future Developments

The results from the statistical method applied to the Livraria Lello staircase are not 100% conclusive. Consider not applying the Hamming window or choosing L values with smaller time steps, such as $L = 1000, 1010, 1020, \dots, 1100$ seconds, for example.

Appendix A

Part I: method 2 (details)

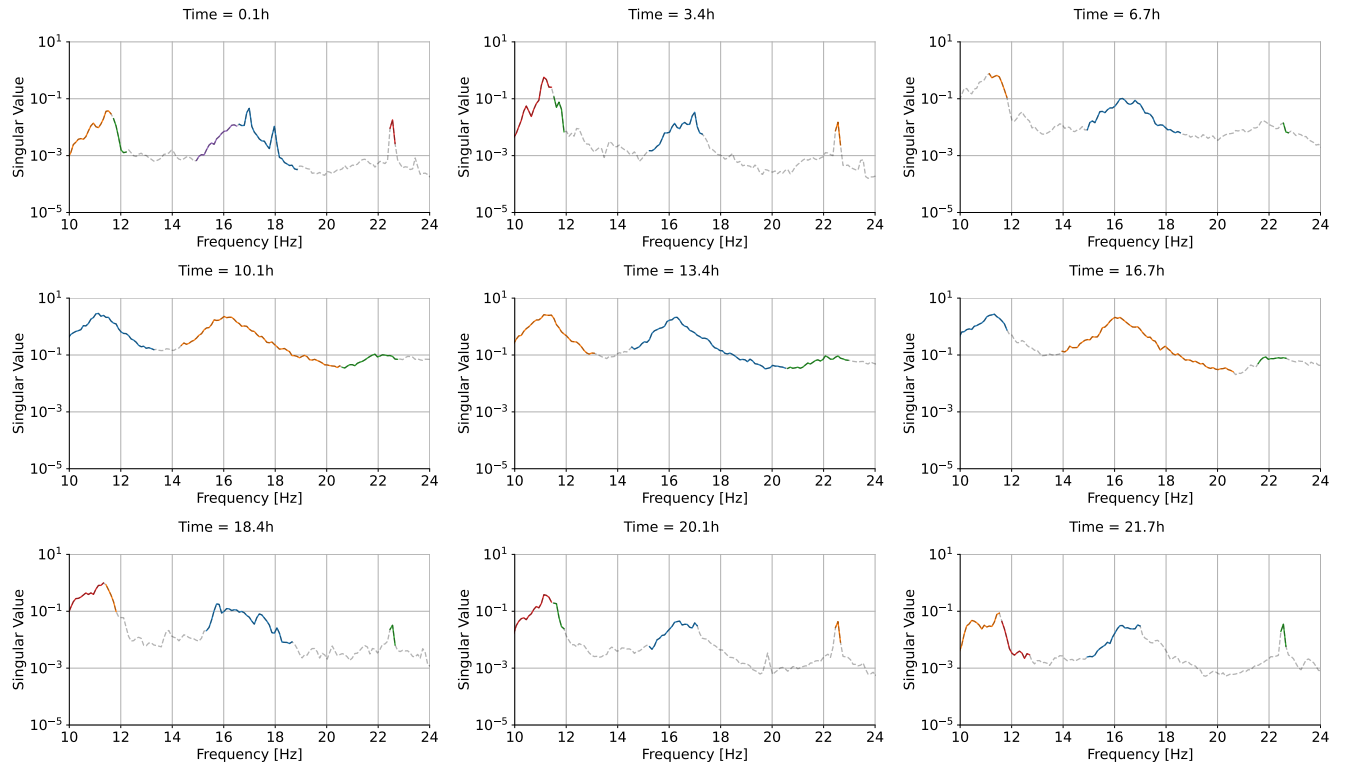


Figure A.1. Evolution of the Singular Values of the PSD matrix through time for the entire day data on July 10, 2023 and a 10 min time window (nperseg = 1024, mac_threshold = 0.95).

Appendix B

”Alfredo” 2-Story Experimental Structure : configurations

1. Test i = 0

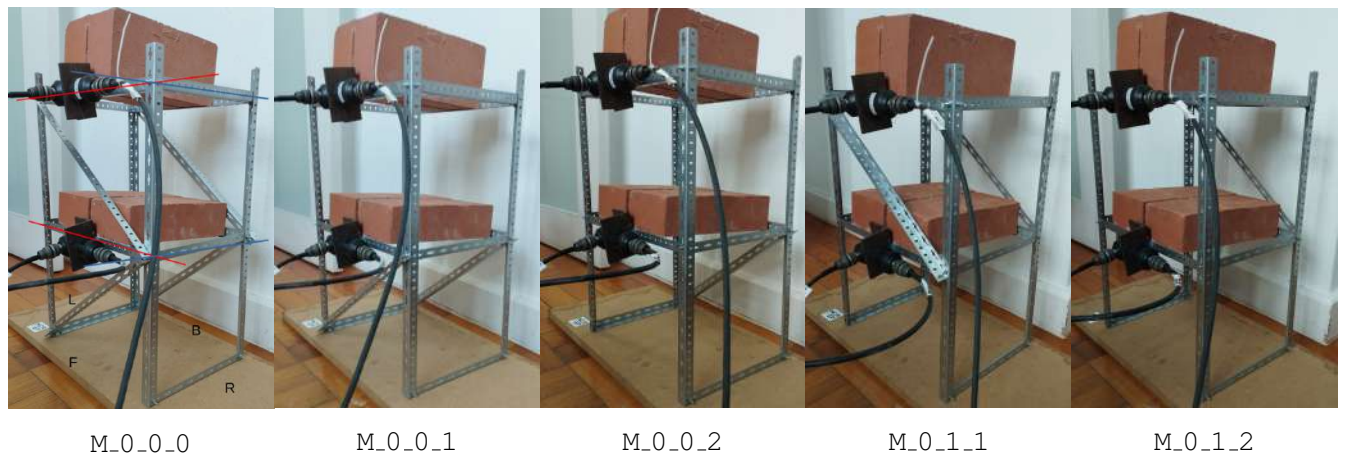


Figure B.1. Different configurations for the first test, in M_0_0_0, the red axis represents the x-direction, and the y-axis represents the y-direction.

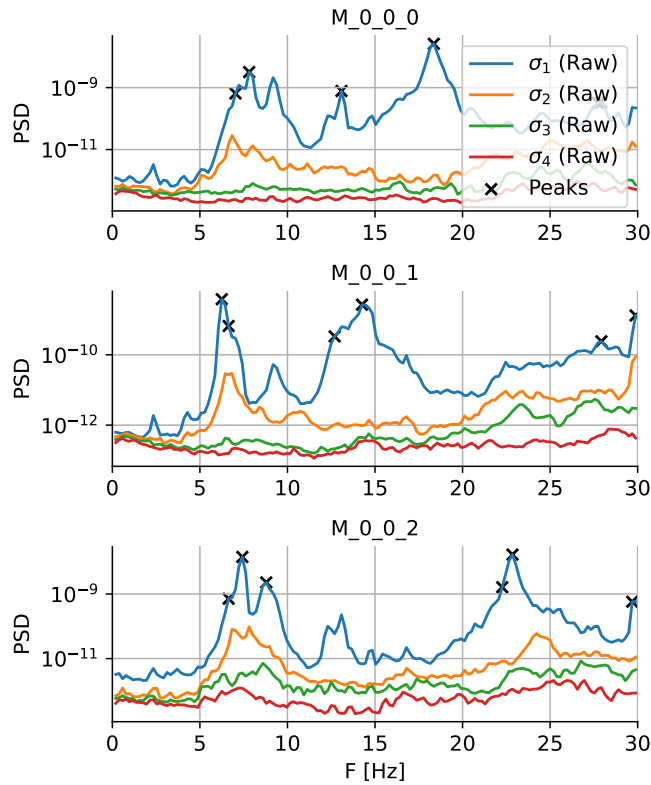


Figure B.2. Evolution of the PSD ($nperseg=1024$) through the iterations of the steps in the **M_0_0_0** test.

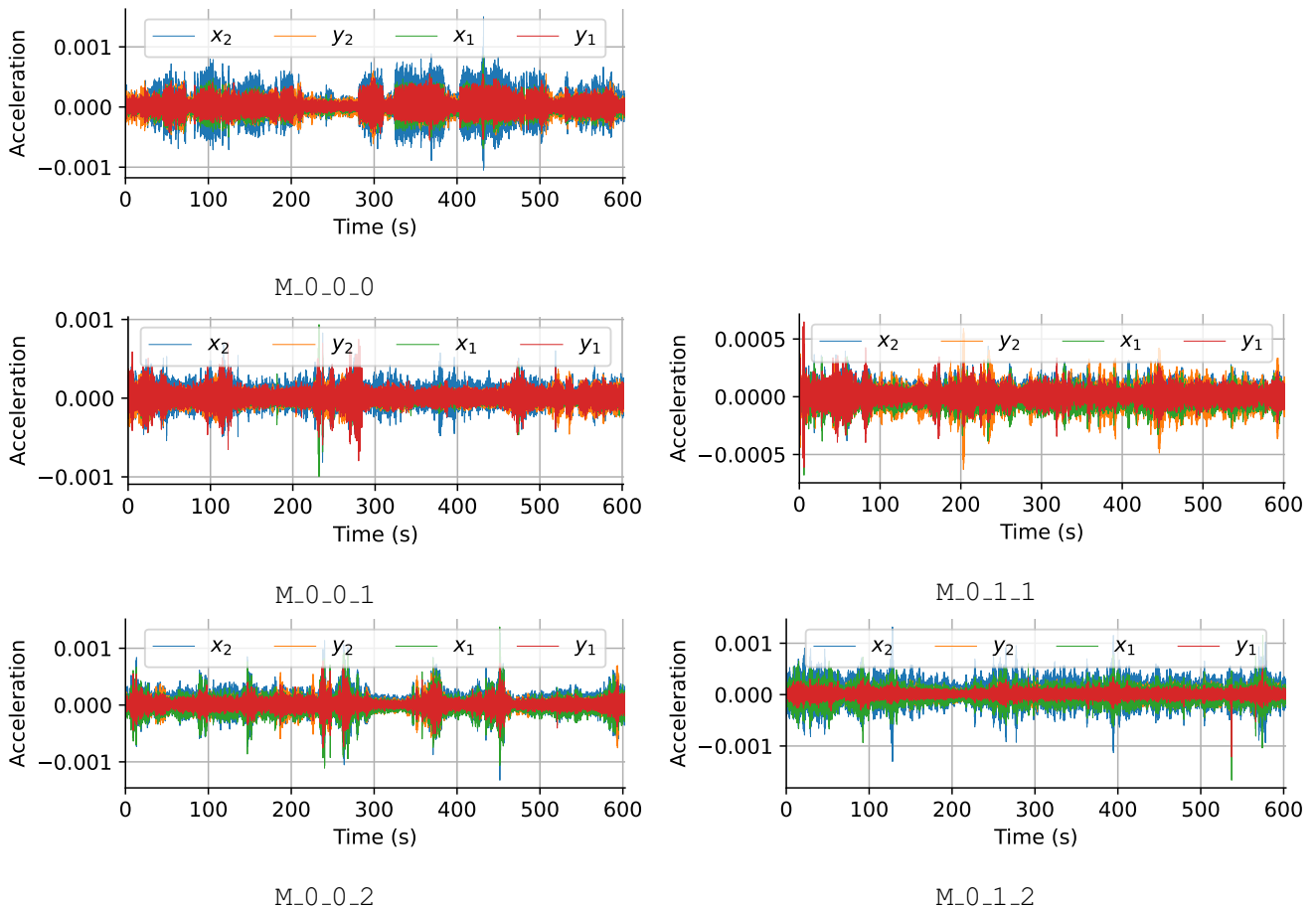


Figure B.3. Obtained accelerograms from the first test.

2. Test i = 1



Figure B.4. Different configurations for the second test. The changes in configuration are not easily visible in the figures, but it can be observed that the number of vertical elements varies.

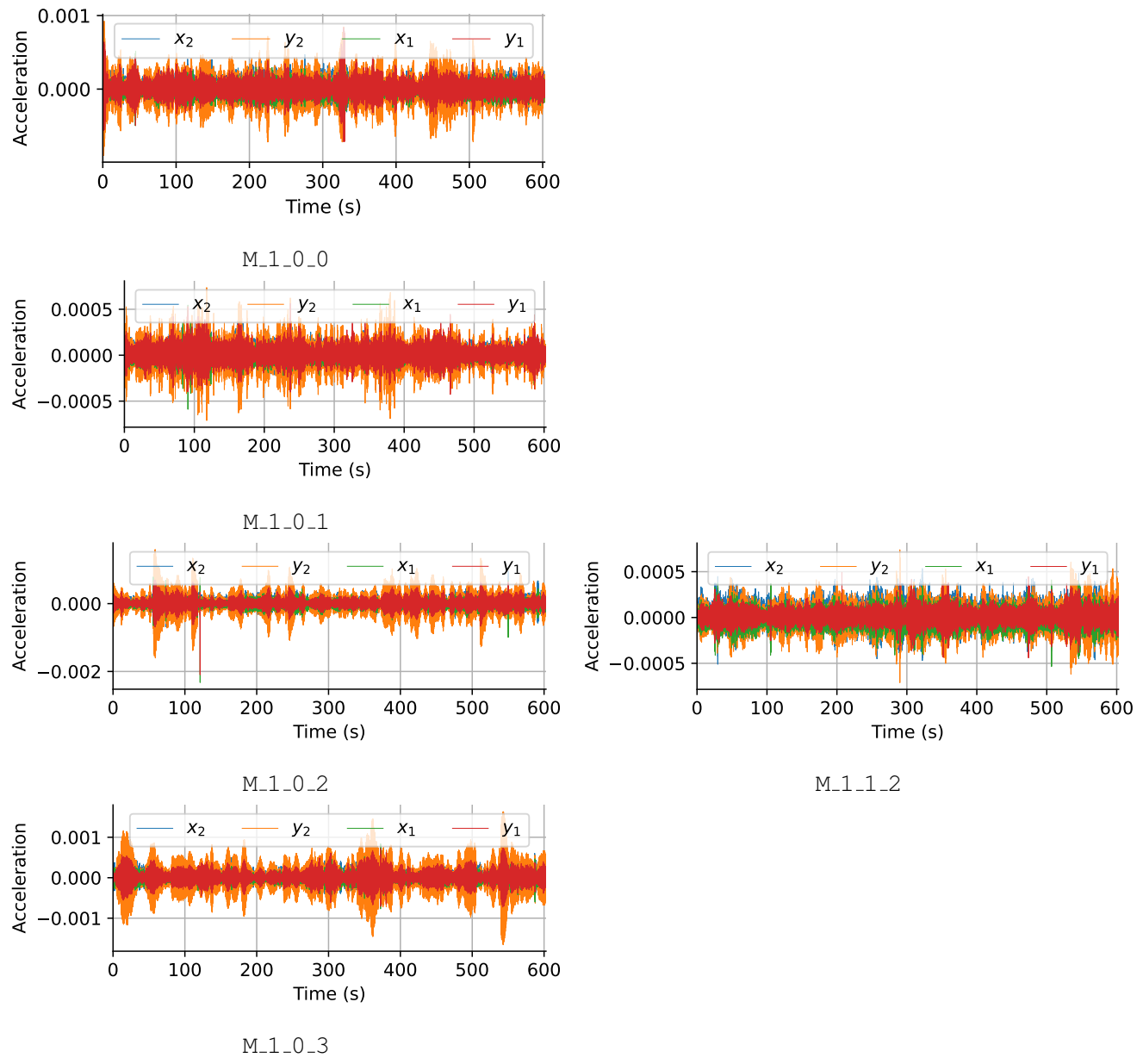


Figure B.5. Obtained accelerograms from the second test.

3. Test i = 1 bis

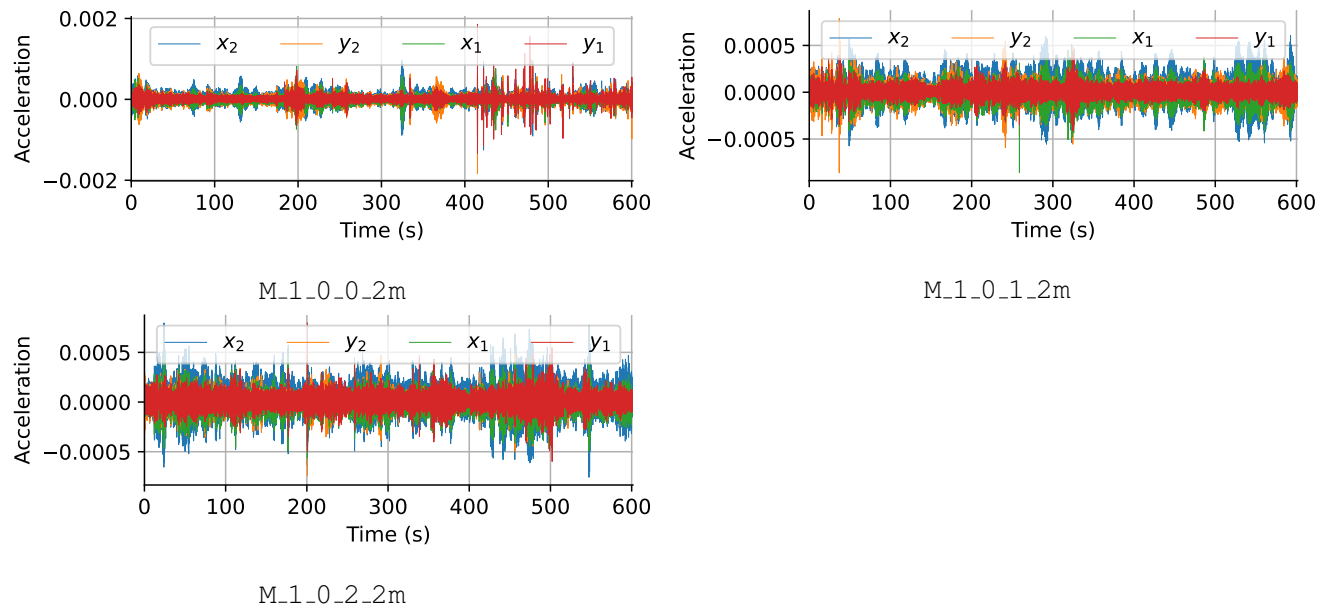


Figure B.6. Accelerograms obtained from the second test with doubled masses.

4. Test i = 2



Figure B.7. Different configurations for the third test.

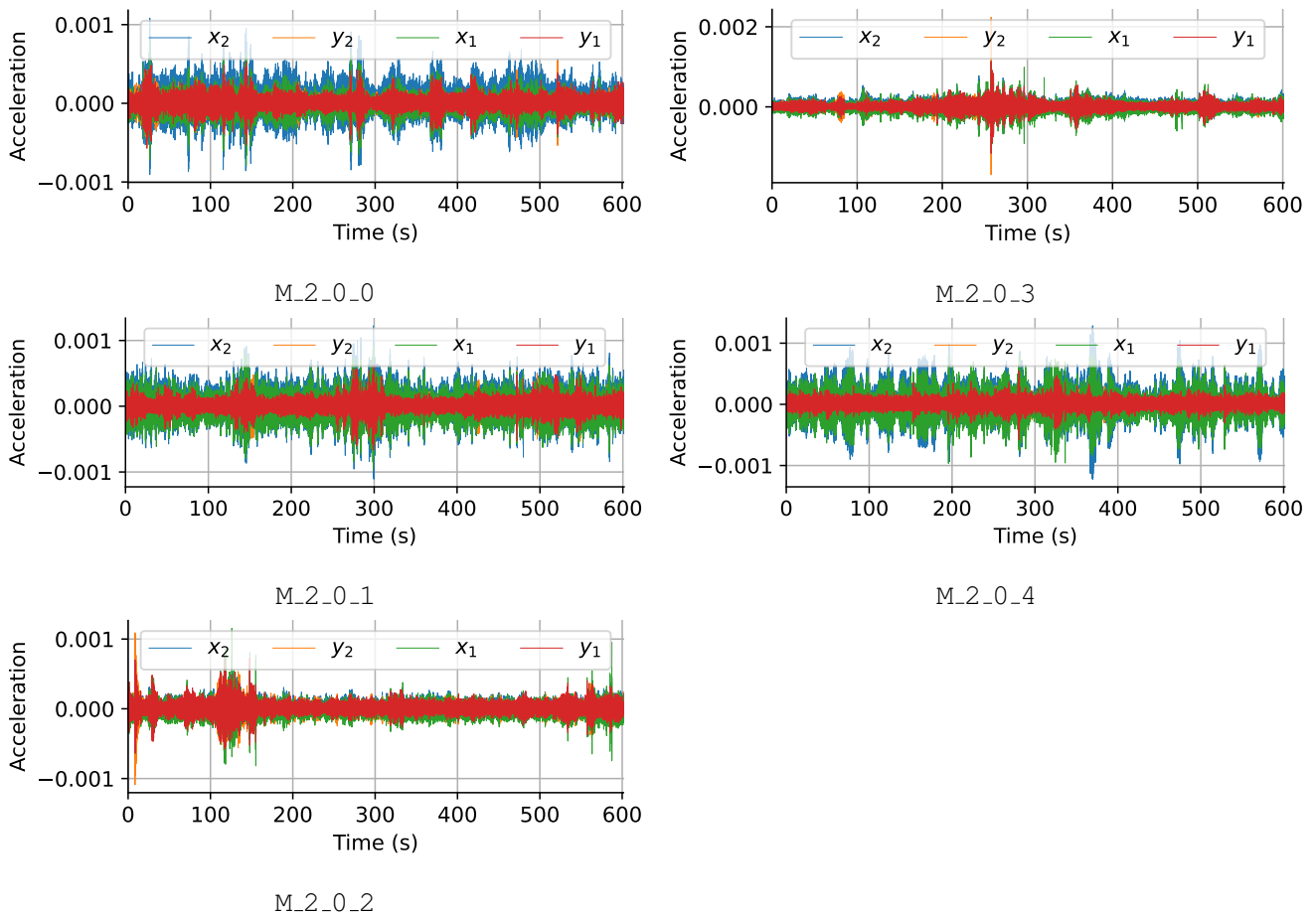


Figure B.8. Obtained accelerograms from the third test.

5. Test i = 3

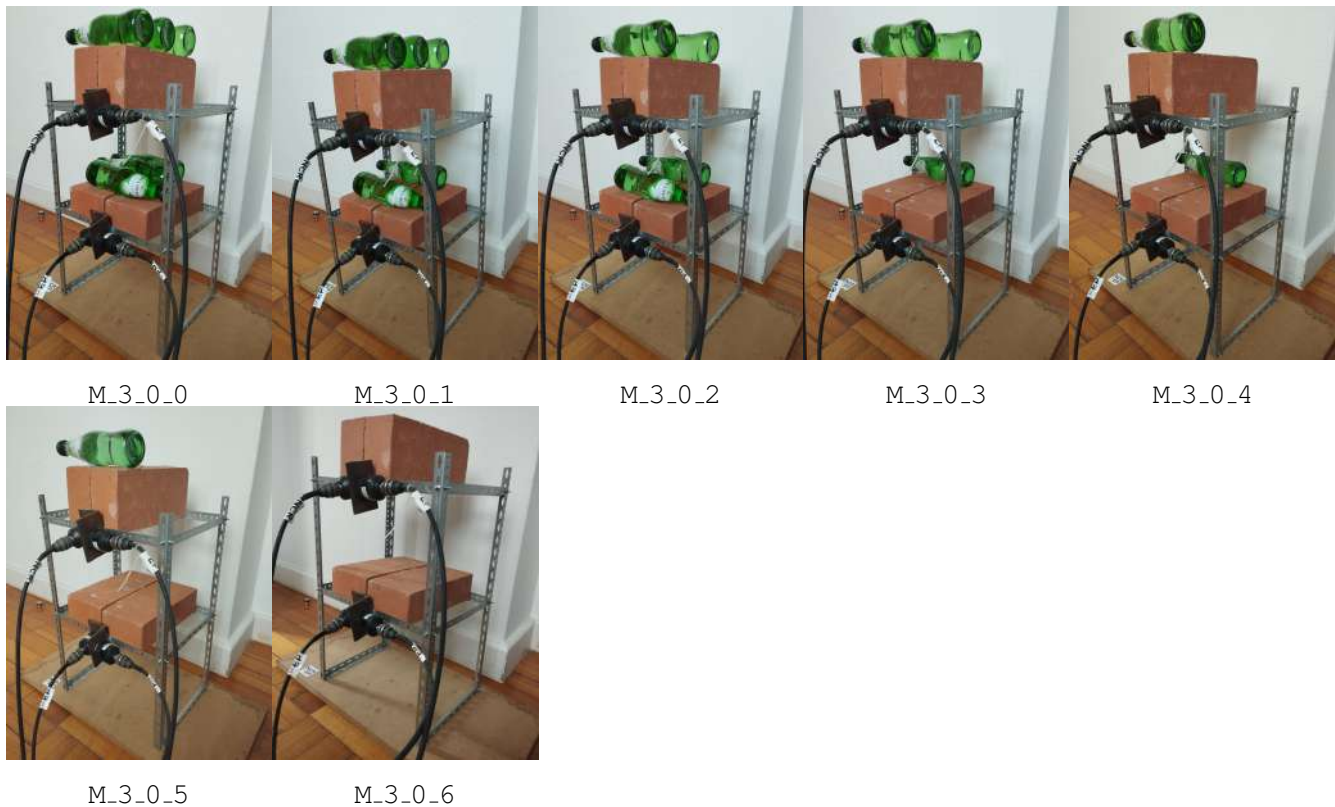


Figure B.9. Different configurations for the fourth test.

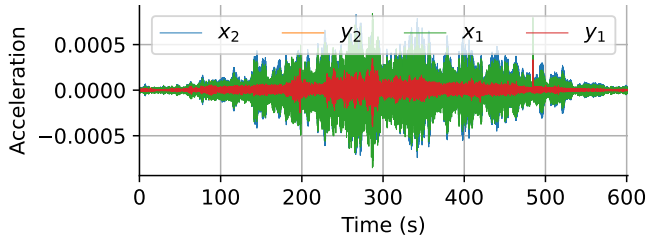


Figure B.10. M_3_0_0

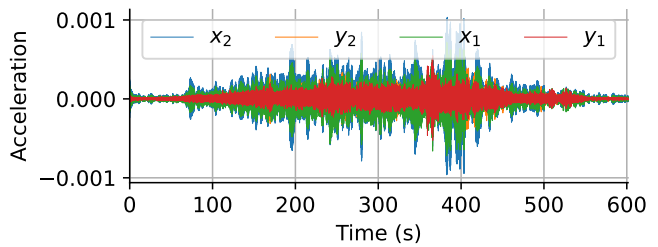
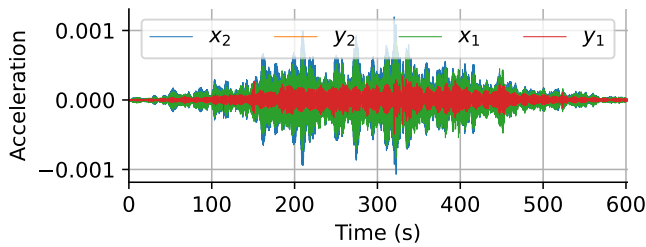
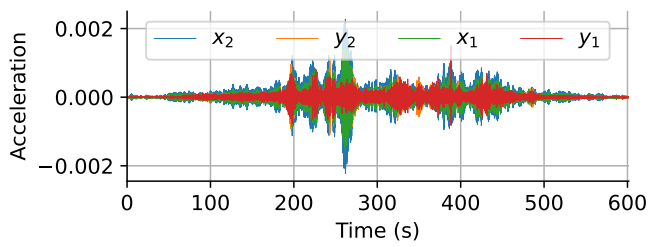


Figure B.11. M_3_0_4



M_3_0_1



M_3_0_5

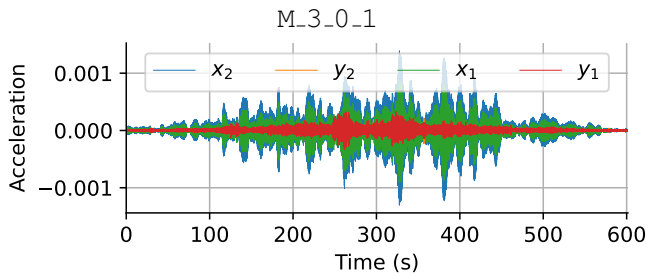
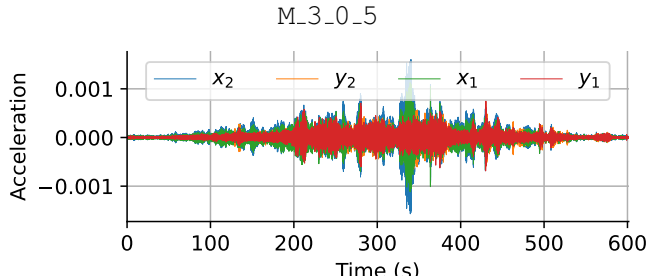


Figure B.12. M_3_0_2



M_3_0_6

Figure B.13. M_3_0_3

Figure B.14. Obtained accelerograms from the fourth test.

Bibliography

- [1] F. M. R. L. de Magalhães, “Operational modal analysis for testing and monitoring of bridges and special structures,” PhD Thesis, Ph.D. dissertation, University of Porto, Porto, Portugal, 2010.
- [2] W.-X. R. Wang-Ji Yan Zhouquan Feng, “New insights into coherence analysis with a view towards extracting structural natural frequencies under operational conditions,” *Measurement*, vol. 77, pp. 187–202, Jan. 2016.
- [3] D. P. Pasca, A. Aloisio, M. M. Rosso, and S. Sotiropoulos, “Pyoma and pyoma_gui: A python module and software for operational modal analysis,” *Software Release*, vol. 1, no. 1, pp. 1–10, Oct. 2022, Original software publication.
- [4] D. Soares, R. d. A. Cardoso, F. d. S. Barbosa, and A. A. Cury, “An automated tool for long-term structural health monitoring based on vibration tests,” *Advances on Testing and Experimentation in Civil Engineering*, vol. Springer Tracts in Civil Engineering, pp. 269–290, 2023. doi: [10.1007/978-3-031-23888-8_12](https://doi.org/10.1007/978-3-031-23888-8_12).
- [5] S. Dyke *et al.*, *Nees: Database for structural control and monitoring benchmark problems*, Accessed: 2024-08-28, 2015. [Online]. Available: <https://datacenterhub.org/resources/257>.